Numerical studies of the transmission of light through a two-dimensional randomly rough interface

Ø.S. Hetland[1], A.A. Maradudin[2], T. Nordam[1], P.A. Letnes[1], J.-P. Banon[1], and I. Simonsen[1]
[1] *Department of Physics, Norwegian University of Science and Technology, NO-7491 Trondheim, Norway and*
[2] *Department of Physics and Astronomy, University of California, Irvine CA 92697, U.S.A.*
(Dated: January 29, 2016)

The transmission of polarized light through a two-dimensional randomly rough interface between two dielectric media has been much less studied, by any approach, than the scattering of light from such an interface. We have derived a reduced Rayleigh equation for the transmission amplitudes when p- or s-polarized light is incident on this type of interface, and have obtained rigorous, purely numerical, nonperturbative solutions of it. The solutions are used to calculate the transmissivity of the interface, the mean differential transmission coefficient, and the full angular distribution of the intensity of the transmitted light. These results are obtained for both the case where the medium of incidence is the optically more dense medium and in the case where it is the optically less dense medium. When the contribution from the scattered field is added to that from the transmitted field, it is found that the results of these calculations satisfy unitarity with an error smaller than 10^{-4}.

I. INTRODUCTION

In the theoretical and experimental studies of the interaction of an electromagnetic wave with a two-dimensional randomly rough dielectric surface, the great majority of them have been devoted to the scattering problem [1–3], and little attention has been paid to studies of the transmission of light through such surfaces. Greffet [4] obtained a reduced Rayleigh equation for the transmission amplitudes in the case where light incident from vacuum is transmitted through a two-dimensional randomly rough interface into a dielectric medium, and obtained a recursion relation for the successive terms in the expansions of the amplitudes in powers of the surface profile function. Kawanishi *et al.* [5] by the use of the stochastic functional approach studied the case where a two-dimensional randomly rough interface between two dielectric media is illuminated by *p*- and *s*-polarized light from either medium. Properties of the light transmitted through, as well as scattered from, the interface were examined. The theoretical approach is perturbative in nature and can be applied only to weakly rough surfaces. Nevertheless, Kawanishi *et al.* obtained several interesting properties of the transmitted light that are associated with the phenomenon of total internal reflection when the medium of transmission was the optically denser medium. These include the appearance of Yoneda peaks in the dependence of the intensity of the transmitted light as a function of the angles of transmission for a fixed value of the angle of incidence. These are sharp asymmetric peaks at the angles of transmission related to the critical angle for total internal reflection, when the medium of transmission is the optically more dense medium. Although well known in the scattering of x-rays from a metal surface [6, 7], the paper by Kawanishi *et al.* apparently marks their first appearance in optics, where they have yet to be observed. Soubret *et al.* [8] also obtained a reduced Rayleigh equation for the transmission amplitudes in the case where light incident from one dielectric medium is transmitted into a second dielectric medium through a two-dimensional randomly rough interface. However, no solutions of this equation were obtained by them.

In this paper we present a theoretical study of the transmission of light through a two-dimensional randomly rough interface between two dielectric media that is free from the limitations and approximations present in the earlier studies of this problem. We obtain a reduced Rayleigh equation for the transmission amplitudes in the case where light incident from a dielectric medium whose dielectric constant is ε_1 is transmitted through a two-dimensional randomly rough interface into a dielectric medium whose dielectric constant is ε_2. The dielectric constant ε_1 can be larger or smaller than the dielectric constant ε_2. Thus, effects associated with total internal reflection are included in the solutions of this equation. Instead of solving the reduced Rayleigh equation as an expansion in powers of the surface profile function, in this work we obtain a rigorous, purely numerical, nonperturbative solution of it. This approach enables us to calculate the transmittance of the system studied, the in-plane co- and cross-polarized, and the out-of-plane co- and cross-polarized scattering contributions to the mean differential transmission coefficient, and the angular dependence of the total scattered intensity, all in a nonperturbative fashion.

II. THE SCATTERING SYSTEM

The system we study in this paper consists of a dielectric medium (medium 1), whose dielectric constant is ε_1, in the region $x_3 > \zeta(\mathbf{x}_\parallel)$, and a dielectric medium (medium 2), whose dielectric constant is ε_2, in the region $x_3 < \zeta(\mathbf{x}_\parallel)$ [Fig. 1]. Here $\mathbf{x}_\parallel = (x_1, x_2, 0)$ is an arbitrary vector in the plane $x_3 = 0$, and we assume that both ε_1 and ε_2 are real, positive, and independent of frequency.

The surface profile function $\zeta(\mathbf{x}_\parallel)$ is assumed to be a single-valued function of $\mathbf{x}_\parallel$ that is differentiable with respect to x_1 and x_2, and constitutes a stationary, zero-mean, isotropic, Gaussian random process defined by

$$\langle \zeta(\mathbf{x}_\parallel)\zeta(\mathbf{x}'_\parallel)\rangle = \delta^2 W(|\mathbf{x}_\parallel - \mathbf{x}'_\parallel|). \tag{1}$$

The angle brackets here and in all that follows denote an average over the ensemble of realizations of the surface profile function. The root-mean-square height of the surface is given by

$$\delta = \langle \zeta^2(\mathbf{x}_\parallel)\rangle^{\frac{1}{2}}. \tag{2}$$

The power spectrum of the surface roughness $g(k_\parallel)$ is defined by

$$g(k_\parallel) = \int \mathrm{d}^2 x_\parallel \; W(x_\parallel) \exp(-\mathrm{i}\mathbf{k}_\parallel \cdot \mathbf{x}_\parallel). \tag{3}$$

We will assume for the normalized surface height autocorrelation function $W(x_\parallel)$ the Gaussian function

$$W(x_\parallel) = \exp\left(-\frac{x_\parallel^2}{a^2}\right). \tag{4}$$

The characteristic length a is the transverse correlation length of the surface roughness. The corresponding power spectrum is given by

$$g(k_\parallel) = \pi a^2 \exp\left(-\frac{k_\parallel^2 a^2}{4}\right). \tag{5}$$

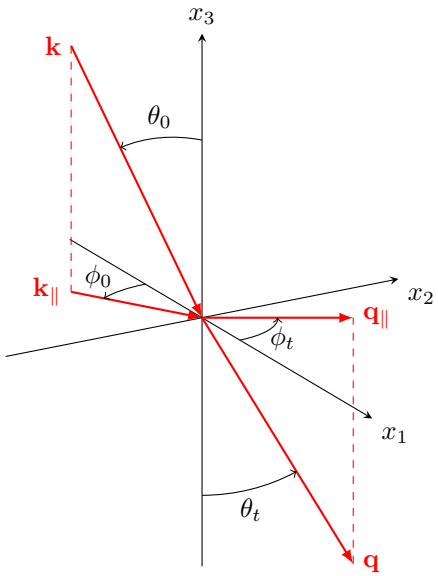

FIG. 1. A sketch of the scattering geometry assumed in this work. The figure also shows the coordinate system used, angles of incidence(θ_0, ϕ_0) and transmission (θ_t, ϕ_t), and the corresponding lateral wavevectors $\mathbf{k}_\parallel$ and $\mathbf{q}_\parallel$, respectively.

III. THE REDUCED RAYLEIGH EQUATION

The interface $x_3 = \zeta(\mathbf{x}_\parallel)$ is illuminated from the region $x_3 > \zeta(\mathbf{x}_\parallel)$ (medium 1) by an electromagnetic wave of frequency ω. The total electric field in this region is the sum of an incoming incident field and an outgoing scattered field,

$$\mathbf{E}^{>}(\mathbf{x}|\omega) = \mathbf{E}_0(\mathbf{k}_\parallel)\exp[\mathrm{i}\mathbf{Q}_0(\mathbf{k}_\parallel)\cdot\mathbf{x}] + \int \frac{\mathrm{d}^2 q_\parallel}{(2\pi)^2}\,\mathbf{A}(\mathbf{q}_\parallel)\exp[\mathrm{i}\mathbf{Q}_1(\mathbf{q}_\parallel)\cdot\mathbf{x}], \tag{6}$$

while the electric field in the region $x_3 < \zeta(\mathbf{x}_\parallel)$ is an outgoing transmitted field,

$$\mathbf{E}^{<}(\mathbf{x}|\omega) = \int \frac{\mathrm{d}^2 q_\parallel}{(2\pi)^2}\,\mathbf{B}(\mathbf{q}_\parallel)\exp[\mathrm{i}\mathbf{Q}_2(\mathbf{q}_\parallel)\cdot\mathbf{x}]. \tag{7}$$

In writing these equations we have introduced the functions

$$\mathbf{Q}_0(\mathbf{k}_\parallel) = \mathbf{k}_\parallel - \alpha_1(k_\parallel)\hat{\mathbf{x}}_3 \tag{8a}$$
$$\mathbf{Q}_1(\mathbf{q}_\parallel) = \mathbf{q}_\parallel + \alpha_1(q_\parallel)\hat{\mathbf{x}}_3 \tag{8b}$$
$$\mathbf{Q}_2(\mathbf{q}_\parallel) = \mathbf{q}_\parallel - \alpha_2(q_\parallel)\hat{\mathbf{x}}_3, \tag{8c}$$

where $(i = 1, 2)$

$$\alpha_i(q_\parallel) = \begin{cases} \sqrt{\varepsilon_i\left(\frac{\omega}{c}\right)^2 - q_\parallel^2}, & q_\parallel \le \sqrt{\varepsilon_i}\,\omega/c \\ \mathrm{i}\sqrt{q_\parallel^2 - \varepsilon_i\left(\frac{\omega}{c}\right)^2}, & q_\parallel > \sqrt{\varepsilon_i}\,\omega/c \end{cases}. \tag{9}$$

Here $\mathbf{k}_\parallel = (k_1, k_2, 0)$, $k_\parallel = \left|\mathbf{k}_\parallel\right|$, and a caret over a vector indicates that it is a unit vector. A time dependence of the field of the form $\exp(-\mathrm{i}\omega t)$ has been assumed, but not indicated explicitly.

The boundary conditions satisfied by these fields at the interface $x_3 = \zeta(\mathbf{x}_\parallel)$ are the continuity of the tangential components of the electric field:

$$\begin{aligned}\mathbf{n}\times\mathbf{E}_0(\mathbf{k}_\parallel)\exp[\mathrm{i}\mathbf{k}_\parallel\cdot\mathbf{x}_\parallel - \mathrm{i}\alpha_1(k_\parallel)\zeta(\mathbf{x}_\parallel)] + \int\frac{\mathrm{d}^2q_\parallel}{(2\pi)^2}\,\mathbf{n}\times\mathbf{A}(\mathbf{q}_\parallel)\exp[\mathrm{i}\mathbf{q}_\parallel\cdot\mathbf{x}_\parallel + \mathrm{i}\alpha_1(q_\parallel)\zeta(\mathbf{x}_\parallel)]\\ = \int\frac{\mathrm{d}^2q_\parallel}{(2\pi)^2}\,\mathbf{n}\times\mathbf{B}(\mathbf{q}_\parallel)\exp[\mathrm{i}\mathbf{q}_\parallel\cdot\mathbf{x}_\parallel - \mathrm{i}\alpha_2(q_\parallel)\zeta(\mathbf{x}_\parallel)];\end{aligned} \tag{10}$$

the continuity of the tangential components of the magnetic field:

$$\begin{aligned}\mathbf{n}\times[\mathrm{i}\mathbf{Q}_0(\mathbf{k}_\parallel)\times\mathbf{E}_0(\mathbf{k}_\parallel)]\exp[\mathrm{i}\mathbf{k}_\parallel\cdot\mathbf{x}_\parallel - \mathrm{i}\alpha_1(k_\parallel)\zeta(\mathbf{x}_\parallel)] + \int\frac{\mathrm{d}^2q_\parallel}{(2\pi)^2}\,\mathbf{n}\times[\mathrm{i}\mathbf{Q}_1(\mathbf{q}_\parallel)\times\mathbf{A}(\mathbf{q}_\parallel)]\exp[\mathrm{i}\mathbf{q}_\parallel\cdot\mathbf{x}_\parallel + \mathrm{i}\alpha_1(q_\parallel)\zeta(\mathbf{x}_\parallel)]\\ = \int\frac{\mathrm{d}^2q_\parallel}{(2\pi)^2}\,\mathbf{n}\times[\mathrm{i}\mathbf{Q}_2(\mathbf{q}_\parallel)\times\mathbf{B}(\mathbf{q}_\parallel)]\exp[\mathrm{i}\mathbf{q}_\parallel\cdot\mathbf{x}_\parallel - \mathrm{i}\alpha_2(q_\parallel)\zeta(\mathbf{x}_\parallel)];\end{aligned} \tag{11}$$

and the continuity of the normal component of the electric displacement:

$$\begin{aligned}\varepsilon_1\mathbf{n}\cdot\mathbf{E}_0(\mathbf{k}_\parallel)\exp[\mathrm{i}\mathbf{k}_\parallel\cdot\mathbf{x}_\parallel - \mathrm{i}\alpha_1(k_\parallel)\zeta(\mathbf{x}_\parallel)] + \varepsilon_1\int\frac{\mathrm{d}^2q_\parallel}{(2\pi)^2}\,\mathbf{n}\cdot\mathbf{A}(\mathbf{q}_\parallel)\exp[\mathrm{i}\mathbf{q}_\parallel\cdot\mathbf{x}_\parallel + \mathrm{i}\alpha_1(q_\parallel)\zeta(\mathbf{x}_\parallel)]\\ = \varepsilon_2\int\frac{\mathrm{d}^2q_\parallel}{(2\pi)^2}\,\mathbf{n}\cdot\mathbf{B}(\mathbf{q}_\parallel)\exp[\mathrm{i}\mathbf{q}_\parallel\cdot\mathbf{x}_\parallel - \mathrm{i}\alpha_2(q_\parallel)\zeta(\mathbf{x}_\parallel)].\end{aligned} \tag{12}$$

The vector $\mathbf{n} \equiv \mathbf{n}(\mathbf{x}_\parallel)$ entering these equations is a vector normal to the surface $x_3 = \zeta(\mathbf{x}_\parallel)$ at each point of it, directed into medium 1:

$$\mathbf{n}(\mathbf{x}_\parallel) = \hat{\mathbf{x}}_3 - \boldsymbol{\nabla}_\parallel\zeta(\mathbf{x}_\parallel) = (-\zeta_1(\mathbf{x}_\parallel), -\zeta_2(\mathbf{x}_\parallel), 1), \tag{13a}$$

with $\boldsymbol{\nabla}_\parallel = (\partial/\partial x_1, \partial/\partial x_2, 0)$, and

$$\zeta_\alpha(\mathbf{x}_\parallel) = \frac{\partial}{\partial x_\alpha}\zeta(\mathbf{x}_\parallel), \qquad \alpha = 1, 2. \tag{13b}$$

Strictly speaking the continuity of the tangential components of the electric and magnetic fields across the interface, Eqs. (10) and (11), are sufficient (and necessary) boundary conditions on electromagnetic fields [9]. Hence, the continuity of the normal components of the electric displacement [Eq. (12)] and the magnetic induction are redundant. However, the inclusion of Eq. (12) enables us to eliminate the scattering amplitude $\mathbf{A}(\mathbf{q}_\parallel)$ from consideration, and thus to obtain an equation that relates the transmission amplitude $\mathbf{B}(\mathbf{q}_\parallel)$ to the amplitude of the incident field $\mathbf{E}_0(\mathbf{k}_\parallel)$. This we do in the following manner.

We take the vector cross product of Eq. (10) with $\varepsilon_1\mathbf{Q}_0(\mathbf{p}_\parallel)\exp[\mathrm{i}\mathbf{p}_\parallel\cdot\mathbf{x}_\parallel + \mathrm{i}\alpha_1(p_\parallel)\zeta(\mathbf{x}_\parallel)]$; then multiply Eq. (11) by $-\mathrm{i}\varepsilon_1\exp[-\mathrm{i}\mathbf{p}_\parallel\cdot\mathbf{x}_\parallel + \mathrm{i}\alpha_1(p_\parallel)\zeta(\mathbf{x}_\parallel)]$; and finally multiply Eq. (12) by $-\mathbf{Q}_0(\mathbf{p}_\parallel)\exp[-\mathrm{i}\mathbf{p}_\parallel\cdot\mathbf{x}_\parallel + \mathrm{i}\alpha_1(p_\parallel)\zeta(\mathbf{x}_\parallel)]$, where $\mathbf{p}_\parallel$ is an arbitrary wave vector in the plane $x_3 = 0$. When we add the three equations obtained in this way, and integrate the sum over $\mathbf{x}_\parallel$ we obtain an equation that can be written in the form

$$\begin{aligned}&\varepsilon_1\Big\{\mathbf{Q}_0(\mathbf{p}_\parallel)\times\Big[\mathbf{V}_E(\mathbf{p}_\parallel|\mathbf{k}_\parallel)\times\mathbf{E}_0(\mathbf{k}_\parallel)\Big] + \mathbf{V}_E(\mathbf{p}_\parallel|\mathbf{k}_\parallel)\times\big[\mathbf{Q}_0(\mathbf{k}_\parallel)\times\mathbf{E}_0(\mathbf{k}_\parallel)\big] - \mathbf{Q}_0(\mathbf{p}_\parallel)\Big[\mathbf{V}_E(\mathbf{p}_\parallel|\mathbf{k}_\parallel)\cdot\mathbf{E}_0(\mathbf{k}_\parallel)\Big]\Big\}\\ &\quad+\varepsilon_1\int\frac{\mathrm{d}^2q_\parallel}{(2\pi)^2}\Big\{\mathbf{Q}_0(\mathbf{p}_\parallel)\times\Big[\mathbf{V}_A(\mathbf{p}_\parallel|\mathbf{q}_\parallel)\times\mathbf{A}(\mathbf{q}_\parallel)\Big] + \mathbf{V}_A(\mathbf{p}_\parallel|\mathbf{q}_\parallel)\times\Big[\mathbf{Q}_1(\mathbf{q}_\parallel)\times\mathbf{A}(\mathbf{q}_\parallel)\Big] - \mathbf{Q}_0(\mathbf{p}_\parallel)\Big[\mathbf{V}_A(\mathbf{p}_\parallel|\mathbf{q}_\parallel)\cdot\mathbf{A}(\mathbf{q}_\parallel)\Big]\Big\}\\ &= \int\frac{\mathrm{d}^2q_\parallel}{(2\pi)^2}\Big\{\varepsilon_1\mathbf{Q}_0(\mathbf{p}_\parallel)\times\Big[\mathbf{V}_B(\mathbf{p}_\parallel|\mathbf{q}_\parallel)\times\mathbf{B}(\mathbf{q}_\parallel)\Big] + \varepsilon_1\mathbf{V}_B(\mathbf{p}_\parallel|\mathbf{q}_\parallel)\times\Big[\mathbf{Q}_2(\mathbf{q}_\parallel)\times\mathbf{B}(\mathbf{q}_\parallel)\Big] - \varepsilon_2\mathbf{Q}_0(\mathbf{p}_\parallel)\Big[\mathbf{V}_B(\mathbf{p}_\parallel|\mathbf{q}_\parallel)\cdot\mathbf{B}(\mathbf{q}_\parallel)\Big]\Big\},\end{aligned} \tag{14}$$

where

$$\mathbf{V}_E(\mathbf{p}_\parallel|\mathbf{k}_\parallel) = \mathbf{V}\Big(-\alpha_1(p_\parallel) + \alpha_1(k_\parallel)|\mathbf{p}_\parallel - \mathbf{k}_\parallel\Big) \tag{15a}$$

$$\mathbf{V}_A(\mathbf{p}_\parallel|\mathbf{q}_\parallel) = \mathbf{V}\Big(-\alpha_1(p_\parallel) - \alpha_1(q_\parallel)|\mathbf{p}_\parallel - \mathbf{q}_\parallel\Big) \tag{15b}$$

$$\mathbf{V}_B(\mathbf{p}_\parallel|\mathbf{q}_\parallel) = \mathbf{V}\Big(-\alpha_1(p_\parallel) + \alpha_2(q_\parallel)|\mathbf{p}_\parallel - \mathbf{q}_\parallel\Big), \tag{15c}$$

with

$$\mathbf{V}(\gamma|\mathbf{Q}_\parallel) = \int \mathrm{d}^2 x_\parallel \; \mathbf{n}(\mathbf{x}_\parallel) \exp\left(-\mathrm{i}\mathbf{Q}_\parallel \cdot \mathbf{x}_\parallel\right) \exp\left[-\mathrm{i}\gamma\zeta(\mathbf{x}_\parallel)\right]. \tag{16a}$$

It is shown in Appendix A that

$$\mathbf{V}(\gamma|\mathbf{Q}_\parallel) = \frac{I(\gamma|\mathbf{Q}_\parallel)}{\gamma}\left(\mathbf{Q}_\parallel + \gamma\hat{\mathbf{x}}_3\right) - (2\pi)^2\,\delta\left(\mathbf{Q}_\parallel\right)\frac{\mathbf{Q}_\parallel}{\gamma}, \tag{16b}$$

where

$$I(\gamma|\mathbf{Q}_\parallel) = \int \mathrm{d}^2 x_\parallel \; \exp\left(-\mathrm{i}\mathbf{Q}_\parallel \cdot \mathbf{x}_\parallel\right) \exp\left[-\mathrm{i}\gamma\zeta(\mathbf{x}_\parallel)\right]. \tag{17}$$

When the results given by Eqs. (15) and (16) are substituted into Eq. (14), the latter becomes

$$\begin{aligned}(2\pi)^2\delta(\mathbf{p}_\parallel - \mathbf{k}_\parallel)2\varepsilon_1 \frac{\mathbf{k}_\parallel \cdot (\mathbf{p}_\parallel - \mathbf{k}_\parallel)}{-\alpha_1(p_\parallel) + \alpha_1(k_\parallel)}\mathbf{E}_0(\mathbf{k}_\parallel) \\ = (\varepsilon_1 - \varepsilon_2)\int \frac{\mathrm{d}^2 q_\parallel}{(2\pi)^2}\,\frac{I(-\alpha_1(p_\parallel) + \alpha_2(q_\parallel)|\mathbf{p}_\parallel - \mathbf{q}_\parallel)}{-\alpha_1(p_\parallel) + \alpha_2(q_\parallel)}\left\{-\varepsilon_1\left(\frac{\omega}{c}\right)^2\mathbf{B}(\mathbf{q}_\parallel) + \left[\mathbf{Q}_0(\mathbf{p}_\parallel)\cdot\mathbf{B}(\mathbf{q}_\parallel)\right]\mathbf{Q}_0(\mathbf{p}_\parallel)\right\}.\end{aligned} \tag{18}$$

In obtaining this result we have used the result that the singular term of $\mathbf{V}_B(\mathbf{p}_\parallel|\mathbf{q}_\parallel)$ does not contribute, since $\mathbf{p}_\parallel = \mathbf{q}_\parallel$ leaves $-\alpha_1(p_\parallel) + \alpha_2(q_\parallel)$ nonzero. If we note that

$$-\alpha_1(p_\parallel) + \alpha_1(k_\parallel) = \frac{\mathbf{k}_\parallel \cdot (\mathbf{p}_\parallel - \mathbf{k}_\parallel)}{\alpha_1(k_\parallel)} + \mathcal{O}\left((\mathbf{p}_\parallel - \mathbf{k}_\parallel)^2\right), \tag{19}$$

the left-hand side of Eq. (18) becomes $(2\pi)^2\delta(\mathbf{p}_\parallel - \mathbf{k}_\parallel)2\varepsilon_1\alpha_1(k_\parallel)\mathbf{E}_0(\mathbf{k}_\parallel)$. Thus we have an equation for the transmission amplitude $\mathbf{B}(\mathbf{q}_\parallel)$ alone:

$$\begin{aligned}\int \frac{\mathrm{d}^2 q_\parallel}{(2\pi)^2}\,\frac{I(-\alpha_1(p_\parallel) + \alpha_2(q_\parallel)|\mathbf{p}_\parallel - \mathbf{q}_\parallel)}{-\alpha_1(p_\parallel) + \alpha_2(q_\parallel)}\left\{-\varepsilon_1\left(\frac{\omega}{c}\right)^2\mathbf{B}(\mathbf{q}_\parallel) + \left[\mathbf{Q}_0(\mathbf{p}_\parallel)\cdot\mathbf{B}(\mathbf{q}_\parallel)\right]\mathbf{Q}_0(\mathbf{p}_\parallel)\right\} \\ = (2\pi)^2\delta(\mathbf{p}_\parallel - \mathbf{k}_\parallel)\frac{2\varepsilon_1\alpha_1(k_\parallel)}{\varepsilon_1 - \varepsilon_2}\mathbf{E}_0(\mathbf{k}_\parallel).\end{aligned} \tag{20}$$

We now write the vectors $\mathbf{E}_0(\mathbf{k}_\parallel)$ and $\mathbf{B}(\mathbf{q}_\parallel)$ in the forms

$$\mathbf{E}_0(\mathbf{k}_\parallel) = \hat{\mathbf{e}}_p^{(i)}(\mathbf{k}_\parallel)E_{0p}(\mathbf{k}_\parallel) + \hat{\mathbf{e}}_s^{(i)}(\mathbf{k}_\parallel)E_{0s}(\mathbf{k}_\parallel), \tag{21a}$$

where

$$\hat{\mathbf{e}}_p^{(i)}(\mathbf{k}_\parallel) = \frac{c}{\sqrt{\varepsilon_1}\omega}\left[\hat{\mathbf{k}}_\parallel\alpha_1(k_\parallel) + \hat{\mathbf{x}}_3 k_\parallel\right] \tag{21b}$$

$$\hat{\mathbf{e}}_s^{(i)}(\mathbf{k}_\parallel) = \hat{\mathbf{x}}_3 \times \hat{\mathbf{k}}_\parallel, \tag{21c}$$

and

$$\mathbf{B}(\mathbf{q}_\parallel) = \hat{\mathbf{e}}_p^{(t)}(\mathbf{q}_\parallel)B_p(\mathbf{q}_\parallel) + \hat{\mathbf{e}}_s^{(t)}(\mathbf{q}_\parallel)B_s(\mathbf{q}_\parallel), \tag{22a}$$

where

$$\hat{\mathbf{e}}_p^{(t)}(\mathbf{q}_\parallel) = \frac{c}{\sqrt{\varepsilon_2}\omega}\left[\hat{\mathbf{q}}_\parallel\alpha_2(q_\parallel) + \hat{\mathbf{x}}_3 q_\parallel\right] \tag{22b}$$

$$\hat{\mathbf{e}}_s^{(t)}(\mathbf{q}_\parallel) = \hat{\mathbf{x}}_3 \times \hat{\mathbf{q}}_\parallel. \tag{22c}$$

In these expressions $E_{0p}(\mathbf{k}_\parallel)$ and $E_{0s}(\mathbf{k}_\parallel)$ are the amplitudes of the p and s polarized components of the incident field with respect to the plane of incidence, defined by the vectors $\hat{\mathbf{k}}_\parallel$ and $\hat{\mathbf{x}}_3$. Similarly, $B_p(\mathbf{q}_\parallel)$ and $B_s(\mathbf{q}_\parallel)$ are the amplitudes of the p and s polarized components of the transmitted field with respect to the plane of transmission defined by the vectors $\hat{\mathbf{q}}_\parallel$ and $\hat{\mathbf{x}}_3$.

Our goal is to express $B_p(\mathbf{q}_\parallel)$ and $B_s(\mathbf{q}_\parallel)$ in terms of $E_{0p}(\mathbf{k}_\parallel)$ and $E_{0s}(\mathbf{k}_\parallel)$. To this end we introduce three mutually perpendicular unit vectors:

$$\hat{\mathbf{a}}_0(\mathbf{p}_\parallel) = \frac{c}{\sqrt{\varepsilon_1}\omega}\left[\hat{\mathbf{p}}_\parallel - \hat{\mathbf{x}}_3\alpha_1(p_\parallel)\right] \tag{23a}$$

$$\hat{\mathbf{a}}_1(\mathbf{p}_\parallel) = \frac{c}{\sqrt{\varepsilon_1}\omega}\left[\hat{\mathbf{p}}_\parallel\alpha_1(p_\parallel) + \hat{\mathbf{x}}_3 p_\parallel\right] \tag{23b}$$

$$\hat{\mathbf{a}}_2(\mathbf{p}_\parallel) = \hat{\mathbf{x}}_3 \times \hat{\mathbf{p}}_\parallel. \tag{23c}$$

We now take the scalar product of Eq. (20) with each of these three unit vectors in turn, after $\mathbf{E}_0(\mathbf{k}_\parallel)$ and $\mathbf{B}(\mathbf{q}_\parallel)$ have been replaced by the right-hand sides of Eq. (21a) and (22a), respectively. The results are:

$$\hat{\mathbf{a}}_0(\mathbf{p}_\parallel)\cdot\text{Eq. (20)}: \qquad 0 = 0; \tag{24a}$$

$$\hat{\mathbf{a}}_1(\mathbf{p}_\parallel)\cdot\text{Eq. (20)}:$$
$$\int \frac{\mathrm{d}^2q_\parallel}{(2\pi)^2}\,\frac{I(-\alpha_1(p_\parallel)+\alpha_2(q_\parallel)|\mathbf{p}_\parallel-\mathbf{q}_\parallel)}{-\alpha_1(p_\parallel)+\alpha_2(q_\parallel)}\Big\{-\sqrt{\frac{\varepsilon_1}{\varepsilon_2}}\left[\alpha_1(p_\parallel)\,\hat{\mathbf{p}}_\parallel\cdot\hat{\mathbf{q}}_\parallel\,\alpha_2(q_\parallel)+p_\parallel q_\parallel\right]B_p(\mathbf{q}_\parallel)$$
$$+\sqrt{\varepsilon_1}\frac{\omega}{c}\alpha_1(p_\parallel)\,\left[\hat{\mathbf{p}}_\parallel\times\hat{\mathbf{q}}_\parallel\right]_3\,B_s(\mathbf{q}_\parallel)\Big\} = (2\pi)^2\delta(\mathbf{p}_\parallel-\mathbf{k}_\parallel)\frac{2\varepsilon_1\alpha_1(k_\parallel)}{\varepsilon_1-\varepsilon_2}E_{0p}(\mathbf{k}_\parallel); \tag{24b}$$

$$\hat{\mathbf{a}}_2(\mathbf{p}_\parallel)\cdot\text{Eq. (20)}:$$
$$\int \frac{\mathrm{d}^2q_\parallel}{(2\pi)^2}\,\frac{I(-\alpha_1(p_\parallel)+\alpha_2(q_\parallel)|\mathbf{p}_\parallel-\mathbf{q}_\parallel)}{-\alpha_1(p_\parallel)+\alpha_2(q_\parallel)}\Big\{-\frac{\varepsilon_1}{\sqrt{\varepsilon_2}}\frac{\omega}{c}\,\left[\hat{\mathbf{p}}_\parallel\times\hat{\mathbf{q}}_\parallel\right]_3\,\alpha_2(q_\parallel)B_p(\mathbf{q}_\parallel)-\varepsilon_1\frac{\omega^2}{c^2}\hat{\mathbf{p}}_\parallel\cdot\hat{\mathbf{q}}_\parallel B_s(\mathbf{q}_\parallel)\Big\}$$
$$= (2\pi)^2\delta(\mathbf{p}_\parallel-\mathbf{k}_\parallel)\frac{2\varepsilon_1\alpha_1(k_\parallel)}{\varepsilon_1-\varepsilon_2}E_{0s}(\mathbf{k}_\parallel). \tag{24c}$$

These equations represent linear relations between $B_{p,s}(\mathbf{q}_\parallel)$ and $E_{0p,s}(\mathbf{k}_\parallel)$ which we write in the form ($\alpha = p, s,\ \beta = p, s$)

$$B_\alpha(\mathbf{q}_\parallel) = \sum_\beta T_{\alpha\beta}(\mathbf{q}_\parallel|\mathbf{k}_\parallel)E_{0\beta}(\mathbf{k}_\parallel). \tag{25}$$

On combining Eqs. (24) and (25) we find that the transmission amplitudes $\{T_{\alpha\beta}(\mathbf{q}_\parallel|\mathbf{k}_\parallel)\}$ are the solutions of the equation

$$\int \frac{\mathrm{d}^2q_\parallel}{(2\pi)^2}\,\frac{I(-\alpha_1(p_\parallel)+\alpha_2(q_\parallel)|\mathbf{p}_\parallel-\mathbf{q}_\parallel)}{-\alpha_1(p_\parallel)+\alpha_2(q_\parallel)}\mathbf{M}(\mathbf{p}_\parallel|\mathbf{q}_\parallel)\mathbf{T}(\mathbf{q}_\parallel|\mathbf{k}_\parallel) = (2\pi)^2\delta(\mathbf{p}_\parallel-\mathbf{k}_\parallel)\frac{2\alpha_1(k_\parallel)}{\varepsilon_2-\varepsilon_1}\mathbf{I}_2, \tag{26}$$

where

$$\mathbf{M}(\mathbf{p}_\parallel|\mathbf{q}_\parallel) = \begin{pmatrix} \frac{1}{\sqrt{\varepsilon_1\varepsilon_2}}[\alpha_1(p_\parallel)\,\hat{\mathbf{p}}_\parallel\cdot\hat{\mathbf{q}}_\parallel\,\alpha_2(q_\parallel)+p_\parallel q_\parallel] & -\frac{1}{\sqrt{\varepsilon_1}}\frac{\omega}{c}\alpha_1(p_\parallel)\,[\hat{\mathbf{p}}_\parallel\times\hat{\mathbf{q}}_\parallel]_3 \\ \frac{1}{\sqrt{\varepsilon_2}}\frac{\omega}{c}[\hat{\mathbf{p}}_\parallel\times\hat{\mathbf{q}}_\parallel]_3\,\alpha_2(q_\parallel) & \frac{\omega^2}{c^2}\,\hat{\mathbf{p}}_\parallel\cdot\hat{\mathbf{q}}_\parallel \end{pmatrix} \tag{27a}$$

$$\mathbf{T}(\mathbf{q}_\parallel|\mathbf{k}_\parallel) = \begin{pmatrix} T_{pp}(\mathbf{q}_\parallel|\mathbf{k}_\parallel) & T_{ps}(\mathbf{q}_\parallel|\mathbf{k}_\parallel) \\ T_{sp}(\mathbf{q}_\parallel|\mathbf{k}_\parallel) & T_{ss}(\mathbf{q}_\parallel|\mathbf{k}_\parallel) \end{pmatrix}, \tag{27b}$$

and

$$\mathbf{I}_2 = \begin{pmatrix} 1 & 0 \\ 0 & 1 \end{pmatrix}. \tag{27c}$$

Equation (26) is the reduced Rayleigh equation for the transmission amplitudes.

IV. THE MEAN DIFFERENTIAL TRANSMISSION COEFFICIENT

The differential transmission coefficient $\partial T/\partial\Omega_t$ is defined such that $(\partial T/\partial\Omega_t)\mathrm{d}\Omega_t$ is the fraction of the total time-averaged flux incident on the interface that is transmitted into the element of solid angle $\mathrm{d}\Omega_t$ about the direction of

transmission (θ_t, ϕ_t). To obtain the mean differential transmission coefficient we first note that the magnitude of the total time-averaged flux incident on the interface is given by

$$\begin{aligned}
P_{\rm inc} &= -{\rm Re}\,\frac{c}{8\pi}\int {\rm d}^2x_\parallel \left\{\mathbf{E}_0^*(\mathbf{k}_\parallel)\times\left[\frac{c}{\omega}\mathbf{Q}_0(\mathbf{k}_\parallel)\times\mathbf{E}_0(\mathbf{k}_\parallel)\right]\right\}_3 \exp\left\{[-{\rm i}\mathbf{Q}_0^*(\mathbf{k}_\parallel)+{\rm i}\mathbf{Q}_0(\mathbf{k}_\parallel)]\cdot\mathbf{x}\right\}\\
&= -{\rm Re}\,\frac{c^2}{8\pi\omega}\int {\rm d}^2x_\parallel\ \left\{\left|\mathbf{E}_0(\mathbf{k}_\parallel)\right|^2\mathbf{Q}_0(\mathbf{k}_\parallel)-\left[\mathbf{E}_0^*(\mathbf{k}_\parallel)\cdot\mathbf{Q}_0(\mathbf{k}_\parallel)\right]\mathbf{E}_0(\mathbf{k}_\parallel)\right\}_3\\
&= {\rm Re}\,\frac{c^2}{8\pi\omega}\int {\rm d}^2x_\parallel\ \alpha_1(k_\parallel)\left|\mathbf{E}_0(\mathbf{k}_\parallel)\right|^2\\
&= S\frac{c^2}{8\pi\omega}\alpha_1(k_\parallel)\left|\mathbf{E}_0(\mathbf{k}_\parallel)\right|^2. \qquad (28)
\end{aligned}$$

In this result S is the area of the x_1x_2 plane covered by the randomly rough surface. The minus sign on the right-hand side of the first equation compensates for the fact that the 3-component of the incident flux is negative, and we have used the fact that $\alpha_1(k_\parallel)$ is real, so that $\mathbf{Q}_0(\mathbf{k}_\parallel)$ is real, and $\mathbf{E}_0^*(\mathbf{k}_\parallel)\cdot\mathbf{Q}_0(\mathbf{k}_\parallel)=0$.

In a similar fashion we note that the total time-averaged transmitted flux is given by

$$\begin{aligned}
P_{\rm trans} =& -{\rm Re}\,\frac{c}{8\pi}\int {\rm d}^2x_\parallel\int\frac{{\rm d}^2q_\parallel}{(2\pi)^2}\int\frac{{\rm d}^2q'_\parallel}{(2\pi)^2}\left\{\mathbf{B}^*(\mathbf{q}_\parallel)\times\left[\frac{c}{\omega}\mathbf{Q}_2(\mathbf{q}'_\parallel)\times\mathbf{B}(\mathbf{q}'_\parallel)\right]\right\}_3\\
&\qquad\times\exp\left\{-{\rm i}(\mathbf{q}_\parallel-\mathbf{q}'_\parallel)\cdot\mathbf{x}_\parallel-{\rm i}\left[\alpha_2(q'_\parallel)-\alpha_2^*(q_\parallel)\right]x_3\right\}\\
=& -{\rm Re}\,\frac{c^2}{8\pi\omega}\int\frac{{\rm d}^2q_\parallel}{(2\pi)^2}\left\{\mathbf{B}^*(\mathbf{q}_\parallel)\times\left[\mathbf{Q}_2(\mathbf{q}_\parallel)\times\mathbf{B}(\mathbf{q}_\parallel)\right]\right\}_3\exp\left[2{\rm Im}\,\alpha_2(q_\parallel)x_3\right]\\
=& -{\rm Re}\,\frac{c^2}{8\pi\omega}\int\frac{{\rm d}^2q_\parallel}{(2\pi)^2}\left\{\left|\mathbf{B}(\mathbf{q}_\parallel)\right|^2\mathbf{Q}_2(\mathbf{q}_\parallel)-\left[\mathbf{B}^*(\mathbf{q}_\parallel)\cdot\mathbf{Q}_2(\mathbf{q}_\parallel)\right]\mathbf{B}(\mathbf{q}_\parallel)\right\}_3\exp[2{\rm Im}\,\alpha_2(q_\parallel)x_3]\\
=& {\rm Re}\,\frac{c^2}{32\pi^3\omega}\int {\rm d}^2q_\parallel\ \left|\mathbf{B}(\mathbf{q}_\parallel)\right|^2\alpha_2(q_\parallel)\exp[2{\rm Im}\,\alpha_2(q_\parallel)x_3]\\
&-{\rm Re}\,\frac{{\rm i}c^4}{16\pi^2\varepsilon_2\omega^3}\int {\rm d}^2q_\parallel\ {\rm Im}\,\alpha_2(q_\parallel)q_\parallel^2\left|B_p(\mathbf{q}_\parallel)\right|^2\exp[2{\rm Im}\,\alpha_2(q_\parallel)x_3]. \qquad (29)
\end{aligned}$$

The integral in the second term is pure imaginary. Thus we have

$$P_{\rm trans}=\frac{c^2}{32\pi^3\omega}\int\limits_{q_\parallel<\sqrt{\varepsilon_2}\frac{\omega}{c}}{\rm d}^2q_\parallel\ \alpha_2(q_\parallel)\left|\mathbf{B}(\mathbf{q}_\parallel)\right|^2. \qquad (30)$$

The vectors $\mathbf{k}_\parallel$ and $\mathbf{q}_\parallel$ can be expressed in terms of the polar and azimuthal angles of incidence (θ_0,ϕ_0) and transmission (θ_t,ϕ_t), respectively, by

$$\mathbf{k}_\parallel=\sqrt{\varepsilon_1}\frac{\omega}{c}\sin\theta_0(\cos\phi_0,\sin\phi_0,0) \qquad (31a)$$

$$\mathbf{q}_\parallel=\sqrt{\varepsilon_2}\frac{\omega}{c}\sin\theta_t(\cos\phi_t,\sin\phi_t,0). \qquad (31b)$$

From these results it follows that

$${\rm d}^2q_\parallel=\varepsilon_2\left(\frac{\omega}{c}\right)^2\cos\theta_t\,{\rm d}\Omega_t, \qquad (32)$$

where ${\rm d}\Omega_t=\sin\theta_t\,{\rm d}\theta_t\,{\rm d}\phi_t$. The total time-averaged transmitted flux becomes

$$P_{\rm trans}=\frac{\varepsilon_2^{3/2}\omega^2}{32\pi^3c}\int{\rm d}\Omega_t\ \cos^2\theta_t\left[\left|B_p(\mathbf{q}_\parallel)\right|^2+\left|B_s(\mathbf{q}_\parallel)\right|^2\right]. \qquad (33)$$

Similarly, the total time averaged incident flux, Eq. (28), becomes

$$P_{\rm inc}=S\frac{\sqrt{\varepsilon_1}c}{8\pi}\cos\theta_0\left[\left|E_{0p}(\mathbf{k}_\parallel)\right|^2+\left|E_{0s}(\mathbf{k}_\parallel)\right|^2\right]. \qquad (34)$$

Thus by definition, the differential transmission coefficient is given by

$$\frac{\partial T}{\partial \Omega_t} = \frac{1}{S}\frac{\varepsilon_2^{3/2}}{\varepsilon_1^{1/2}}\left(\frac{\omega}{2\pi c}\right)^2 \frac{\cos^2\theta_t}{\cos\theta_0}\frac{\left|B_p(\mathbf{q}_\parallel)\right|^2 + \left|B_s(\mathbf{q}_\parallel)\right|^2}{\left|E_{0p}(\mathbf{k}_\parallel)\right|^2 + \left|E_{0s}(\mathbf{k}_\parallel)\right|^2}. \tag{35}$$

When we combine this result with Eq. (25) we find that the contribution to the differential transmission coefficient when an incident plane wave of polarization β, the projection of whose wave vector on the mean scattering plane is $\mathbf{k}_\parallel$, is transmitted into a plane wave of polarization α, the projection of whose wave vector on the mean scattering plane is $\mathbf{q}_\parallel$, is given by

$$\frac{\partial T_{\alpha\beta}(\mathbf{q}_\parallel|\mathbf{k}_\parallel)}{\partial \Omega_t} = \frac{1}{S}\frac{\varepsilon_2^{3/2}}{\varepsilon_1^{1/2}}\left(\frac{\omega}{2\pi c}\right)^2 \frac{\cos^2\theta_t}{\cos\theta_0}\left|T_{\alpha\beta}(\mathbf{q}_\parallel|\mathbf{k}_\parallel)\right|^2. \tag{36}$$

Since we are considering the transmission of light through a randomly rough interface, it is the average of this function over the ensemble of realizations of the surface profile function that we need to calculate. This is the mean differential transmission coefficient, which is defined by

$$\left\langle \frac{\partial T_{\alpha\beta}(\mathbf{q}_\parallel|\mathbf{k}_\parallel)}{\partial \Omega_t}\right\rangle = \frac{1}{S}\frac{\varepsilon_2^{3/2}}{\varepsilon_1^{1/2}}\left(\frac{\omega}{2\pi c}\right)^2 \frac{\cos^2\theta_t}{\cos\theta_0}\left\langle \left|T_{\alpha\beta}(\mathbf{q}_\parallel|\mathbf{k}_\parallel)\right|^2\right\rangle. \tag{37}$$

If we write the transmission amplitude $T_{\alpha\beta}(\mathbf{q}_\parallel|\mathbf{k}_\parallel)$ as the sum of its mean value and the fluctuation from this mean,

$$T_{\alpha\beta}(\mathbf{q}_\parallel|\mathbf{k}_\parallel) = \left\langle T_{\alpha\beta}(\mathbf{q}_\parallel|\mathbf{k}_\parallel)\right\rangle + \left[T_{\alpha\beta}(\mathbf{q}_\parallel|\mathbf{k}_\parallel) - \left\langle T_{\alpha\beta}(\mathbf{q}_\parallel|\mathbf{k}_\parallel)\right\rangle\right], \tag{38}$$

then each of these two terms contributes separately to the mean differential transmission coefficient,

$$\left\langle \frac{\partial T_{\alpha\beta}(\mathbf{q}_\parallel|\mathbf{k}_\parallel)}{\partial \Omega_t}\right\rangle = \left\langle \frac{\partial T_{\alpha\beta}(\mathbf{q}_\parallel|\mathbf{k}_\parallel)}{\partial \Omega_t}\right\rangle_{\rm coh} + \left\langle \frac{\partial T_{\alpha\beta}(\mathbf{q}_\parallel|\mathbf{k}_\parallel)}{\partial \Omega_t}\right\rangle_{\rm incoh}, \tag{39}$$

where

$$\left\langle \frac{\partial T_{\alpha\beta}(\mathbf{q}_\parallel|\mathbf{k}_\parallel)}{\partial \Omega_t}\right\rangle_{\rm coh} = \frac{1}{S}\frac{\varepsilon_2^{3/2}}{\varepsilon_1^{1/2}}\left(\frac{\omega}{2\pi c}\right)^2 \frac{\cos^2\theta_t}{\cos\theta_0}\left|\langle T_{\alpha\beta}(\mathbf{q}_\parallel|\mathbf{k}_\parallel)\rangle\right|^2 \tag{40}$$

and

$$\begin{aligned}\left\langle \frac{\partial T_{\alpha\beta}(\mathbf{q}_\parallel|\mathbf{k}_\parallel)}{\partial \Omega_t}\right\rangle_{\rm incoh} &= \frac{1}{S}\frac{\varepsilon_2^{3/2}}{\varepsilon_1^{1/2}}\left(\frac{\omega}{2\pi c}\right)^2 \frac{\cos^2\theta_t}{\cos\theta_0}\left[\left\langle \left|T_{\alpha\beta}(\mathbf{q}_\parallel|\mathbf{k}_\parallel) - \langle T_{\alpha\beta}(\mathbf{q}_\parallel|\mathbf{k}_\parallel)\rangle\right|^2\right\rangle\right] \\ &= \frac{1}{S}\frac{\varepsilon_2^{3/2}}{\varepsilon_1^{1/2}}\left(\frac{\omega}{2\pi c}\right)^2 \frac{\cos^2\theta_t}{\cos\theta_0}\left[\left\langle \left|T_{\alpha\beta}(\mathbf{q}_\parallel|\mathbf{k}_\parallel)\right|^2\right\rangle - \left|\left\langle T_{\alpha\beta}(\mathbf{q}_\parallel|\mathbf{k}_\parallel)\right\rangle\right|^2\right].\end{aligned} \tag{41}$$

The first contribution describes the refraction of the incident field, while the second contribution describes the diffuse transmission.

V. TRANSMISSIVITY AND TRANSMITTANCE

To obtain the transmissivity of the two-dimensional randomly rough interface we start with the result that

$$\langle T_{\alpha\beta}(\mathbf{q}_\parallel|\mathbf{k}_\parallel)\rangle = (2\pi)^2\delta(\mathbf{q}_\parallel - \mathbf{k}_\parallel)\delta_{\alpha\beta}T_\alpha(k_\parallel). \tag{42}$$

The presence of the delta function is due to the stationarity of the randomly rough surface; the Kronecker symbol $\delta_{\alpha\beta}$ arises from the conservation of angular momentum in the transmission process; and the result that $T_\alpha(k_\parallel)$ depends on $\mathbf{k}_\parallel$ only through its magnitude is due to the isotropy of the random roughness.

With the result given by Eq. (42), the expression for $\langle \partial T_{\alpha\beta}(\mathbf{q}_\parallel|\mathbf{k}_\parallel)/\partial\Omega_t\rangle_{\rm coh}$ given by Eq. (40), becomes

$$\left\langle \frac{\partial T_{\alpha\alpha}(\mathbf{q}_\parallel|\mathbf{k}_\parallel)}{\partial \Omega_t}\right\rangle_{\rm coh} = \frac{\varepsilon_2^{3/2}}{\varepsilon_1^{1/2}}\left(\frac{\omega}{c}\right)^2 \frac{\cos^2\theta_t}{\cos\theta_0}\left|T_\alpha(k_\parallel)\right|^2\,\delta(\mathbf{q}_\parallel - \mathbf{k}_\parallel), \tag{43}$$

where we have used the result

$$[(2\pi)^2\delta(\mathbf{q}_\parallel-\mathbf{k}_\parallel)]^2=(2\pi)^2\delta(\mathbf{0})\,(2\pi)^2\delta(\mathbf{q}_\parallel-\mathbf{k}_\parallel)=S(2\pi)^2\delta(\mathbf{q}_\parallel-\mathbf{k}_\parallel) \tag{44}$$

in obtaining this expression. We next use the result

$$\delta(\mathbf{q}_\parallel-\mathbf{k}_\parallel)=\frac{1}{k_\parallel}\delta(q_\parallel-k_\parallel)\,\delta(\phi_t-\phi_0)=\frac{1}{\sqrt{\varepsilon_1\varepsilon_2}}\left(\frac{c}{\omega}\right)^2\frac{\delta(\theta_t-\Theta_t)\,\delta(\phi_t-\phi_0)}{\sin\theta_0\cos\Theta_t} \tag{45}$$

to obtain

$$\left\langle\frac{\partial T_{\alpha\alpha}(\mathbf{q}_\parallel|\mathbf{k}_\parallel)}{\partial\Omega_t}\right\rangle_{\rm coh}=\frac{\varepsilon_2}{\varepsilon_1}\frac{\cos\Theta_t}{\sin\theta_0\cos\theta_0}\left|T_\alpha(k_\parallel)\right|^2\delta(\theta_t-\Theta_t)\,\delta(\phi_t-\phi_0), \tag{46}$$

where the the polar angle for the specular direction of transmission has been denoted

$$\Theta_t\equiv\arcsin\left(\sqrt{\frac{\varepsilon_1}{\varepsilon_2}}\sin\theta_0\right). \tag{47}$$

The transmissivity, $\mathcal{T}_\alpha(\theta_0)$, for light of α polarization is defined by

$$\begin{aligned}\mathcal{T}_\alpha(\theta_0)&=\int_0^{\frac{\pi}{2}}\mathrm{d}\theta_t\,\sin\theta_t\int_{-\pi}^{\pi}\mathrm{d}\phi_t\left\langle\frac{T_{\alpha\alpha}(\mathbf{q}_\parallel|\mathbf{k}_\parallel)}{\partial\Omega_t}\right\rangle_{\rm coh}\\&=\frac{\varepsilon_2}{\varepsilon_1}\frac{\cos\Theta_t\sin\Theta_t}{\sin\theta_0\cos\theta_0}\left|T_\alpha(k_\parallel)\right|^2\int_0^{\frac{\pi}{2}}\mathrm{d}\theta_t\,\delta(\theta_t-\Theta_t)\\&=\begin{cases}\sqrt{\dfrac{\varepsilon_2}{\varepsilon_1}}\dfrac{\cos\Theta_t}{\cos\theta_0}\left|T_\alpha(k_\parallel)\right|^2, & 0<\sqrt{\varepsilon_1/\varepsilon_2}\sin\theta_0<1\\0, & \text{otherwise}\end{cases}.\end{aligned} \tag{48}$$

In writing this expression we have used the result that $\sin\Theta_t=\sqrt{\varepsilon_1/\varepsilon_2}\sin\theta_0$, and, that $\sin\theta_0$ is a monotonically increasing function of θ_0 for $0^\circ<\theta_0<90^\circ$, and so therefore is $\sin\Theta_t$. We see from Eq. (48) that when $\varepsilon_1>\varepsilon_2$ the transmissivity is nonzero for angles of incidence satisfying $0<\theta_0<\arcsin(\sqrt{\varepsilon_2/\varepsilon_1})$, and vanishes for angles of incidence satisfying $\arcsin(\sqrt{\varepsilon_2/\varepsilon_1})<\theta_0<\pi/2$. This result is a consequence for transmission of the existence of a critical angle for total internal reflection, namely $\theta_0^\star=\arcsin(\sqrt{\varepsilon_2/\varepsilon_1})$. In the case where $\varepsilon_1<\varepsilon_2$, the transmissivity is nonzero in the entire range of angles of incidence, $0<\theta_0<\pi/2$. **NOTE: We seem to have several critical angles**: Fix this.

The function $T_\alpha(k_\parallel)$ is obtained from Eq. (42), with the aid of the result that $(2\pi)^2\delta(\mathbf{0})=S$, in the form

$$T_\alpha(k_\parallel)=T_\alpha\left(\sqrt{\varepsilon_1}\frac{\omega}{c}\sin\theta_0\right)=\frac{1}{S}\left\langle T_{\alpha\alpha}(\mathbf{k}_\parallel|\mathbf{k}_\parallel)\right\rangle. \tag{49}$$

In addition to the transmissivity (48) that only depends on the co-polarized light transmitted coherently by the rough interface, it is also of interest to introduce the transmittance for light of β polarization defined as

$$\mathscr{T}_\beta(\theta_0)=\sum_{\alpha=\rm p,s}\mathscr{T}_{\alpha\beta}(\theta_0), \tag{50a}$$

where

$$\mathscr{T}_{\alpha\beta}(\theta_0)=\int_0^{\frac{\pi}{2}}\mathrm{d}\theta_t\,\sin\theta_t\int_{-\pi}^{\pi}\mathrm{d}\phi_t\left\langle\frac{T_{\alpha\beta}(\mathbf{q}_\parallel|\mathbf{k}_\parallel)}{\partial\Omega_t}\right\rangle. \tag{50b}$$

The transmittance measures the fraction of the power flux incident on the rough surface that was transmitted through it. In light of Eq. (39), the transmittance obtains contributions from light that has been transmitted coherently as well as incoherently through the rough interface, $\mathscr{T}_\beta(\theta_0)=\mathscr{T}_\beta(\theta_0)_{\rm coh}+\mathscr{T}_\beta(\theta_0)_{\rm incoh}$, and both co- and cross-polarized transmitted light contribute to it. Moreover, with Eq. (48), and since cross-polarized coherently transmitted light is not allowed [see Eq. (42)], the coherent contribution to transmittance for light of β polarization equals the transmissivity for light of β polarization; $\mathscr{T}_\beta(\theta_0)_{\rm coh}=\mathcal{T}_\beta(\theta_0)$. Therefore, Eq. (50a) can be written in the form

$$\mathscr{T}_\beta(\theta_0)=\mathcal{T}_\beta(\theta_0)+\sum_{\alpha=\rm p,s}\mathscr{T}_{\alpha\beta}(\theta_0)_{\rm incoh}. \tag{51}$$

It remains to remark that in cases where the incident light is not purely p- or s-polarized, the transmittance and transmissivity of the optical system will have to be calculated on the basis of weighted sums of the expressions in Eqs. (48) and (50) where the weights reflect the fraction of p and s polarization associated with the incident light.

VI. RESULTS AND DISCUSSIONS

Calculations were carried out for two-dimensional randomly rough dielectric surfaces defined by an isotropic Gaussian height distribution of rms height $\delta = \lambda/20$ and an isotropic Gaussian correlation function of lateral correlation length $a = \lambda/4$. The incident light consisted of a p- or s-polarized plane wave of wavelength λ (in vacuum) and well-defined angles of incidence (θ_0, ϕ_0). At this wavelength the dielectric constant of the dielectric medium was assumed to be $\varepsilon = 2.6869$; other than a potential dependence of ε on λ, no explicit wavelength dependence was assumed in the simulations. The azimuthal angle of incidence was $\phi_0 = 0^\circ$ in all simulation results presented in this work; this choice for ϕ_0 is somewhat arbitrary, since, due to the isotropy of the roughness, another choice of ϕ_0 can be obtained from the results presented here by a trivial rotation. Moreover, the surfaces covered a square region of the x_1x_2 plane of edge L, giving an area $S = L^2 = 25\lambda \times 25\lambda$. Realizations of the surface profile function were generated [11, 12] in this region on a grid of $N_x \times N_x = 321 \times 321$ points. With these spatial parameters, the corresponding momentum space parameters used in the simulations were $\Delta q = 2\pi/L$ for the discretization intervals in momentum space, and the largest momentum value that can be resolved is given by $\mathcal{Q} = \Delta q \lfloor N_x/2 \rfloor$ where $\lfloor \cdot \rfloor$ denotes the floor function [10]. In the simulations, we used $\mathcal{Q} = 6.4\omega/c$, and for the expansions of the integrands of the $I(\gamma|\mathbf{Q}_\parallel)$-integrals, we used the first $\mathcal{N} = 20$ terms.

The reduced Rayleigh equation (26) was solved by the method described in detail in Ref. 2 so only a summary of this method will be presented here. A realization of the surface profile function was generated on a grid of $N_x \times N_x$ points within a square region of the x_1x_2 plane of edge L. In evaluating the $\mathbf{q}_\parallel$ integral in Eq. (26), the infinite limits of integration were replaced by finite limits $|\mathbf{q}_\parallel| < \mathcal{Q}/2$, and the integration was carried out by a two-dimensional version of the extended midpoint rule [10, p. 161] applied to a grid in the q_1q_2 plane which is determined by the Nyquist sampling theorem [10, p. 605] and the properties of the discrete Fourier transform [2]. The function $I(\gamma|\mathbf{q}_\parallel)$ was evaluated by expanding the integrand in Eq. (17) in powers of $\zeta(\mathbf{x}_\parallel)$ and calculating the Fourier transform of $\zeta^n(\mathbf{x}_\parallel)$ by the fast Fourier transform [2]. The resulting matrix equations were solved by LU factorization and backsubstituting.

These calculations were carried out for a large number N_p of realizations of the surface profile function $\zeta(\mathbf{x}_\parallel)$ for an incident field of p or s polarization. For each realization the transmission amplitude $T_{\alpha\beta}(\mathbf{q}_\parallel|\mathbf{k}_\parallel)$ and its squared modulus $|T_{\alpha\beta}(\mathbf{q}_\parallel|\mathbf{k}_\parallel)|^2$ were obtained. An arithmetic average of the N_p results for these quantities yielded the mean values $\langle T_{\alpha\beta}(\mathbf{q}_\parallel\mathbf{k}_\parallel)\rangle$ and $\langle |T_{\alpha\beta}(\mathbf{q}_\parallel|\mathbf{k}_\parallel)|^2\rangle$ entering Eq. (41) for the mean differential transmission coefficient, and related quantities. [see Eqs. (49) and (51)]

A. Normal incidence

In Fig. 2 we display the mean differential transmission coefficient in the plane of incidence as a function of the polar angle of transmission when the random surface is illuminated from the vacuum at normal incidence by p- and s-polarized light, Fig. 2(a), and when it is illuminated from the dielectric medium Fig. 2(b). Only results for in-plane $[\mathbf{q}_\parallel \parallel \mathbf{k}_\parallel]$ co-polarized transmission are presented because in-plane cross-polarized transmission is suppressed due to the absence of contribution from single-scattering processes. An ensemble of 7500 realizations of the surface profile function was used to produce the averaged results presented in each of these figures. From Fig. 2(a) it is observed that the curves display both maxima and minima in the $p \to p$ transmission spectrum, and peaks in the $s \to s$ transmission spectrum. In contrast, the curves presented in Fig. 2(b) are featureless, and are nearly identical.

The presence of these features, and other in subsequent figures, can be understood if we calculate the contribution to the mean differential transmission coefficient from the light transmitted incoherently through the random interface as an expansion in powers of the surface profile function. This calculation, outlined in Appendix B, yields the result that to lowest nonzero order in $\zeta(\mathbf{x}_\parallel)$ we have

$$\left\langle \frac{\partial T_{pp}(\mathbf{q}_\parallel|\mathbf{k}_\parallel)}{\partial \Omega_t} \right\rangle_{\text{incoh}} = \frac{\delta^2}{\pi^2}(\varepsilon_2 - \varepsilon_1)^2 \varepsilon_1^{1/2} \varepsilon_2^{5/2} \left(\frac{\omega}{c}\right)^2 \frac{\cos^2\theta_t}{\cos\theta_0} g(|\mathbf{q}_\parallel - \mathbf{k}_\parallel|) \times \frac{1}{|d_p(q_\parallel)|^2} \left| \alpha_1(q_\parallel)(\hat{\mathbf{q}}_\parallel \cdot \hat{\mathbf{k}}_\parallel)\alpha_2(k_\parallel) + q_\parallel k_\parallel \right|^2 \frac{\alpha_1^2(k_\parallel)}{|d_p(k_\parallel)|^2} \tag{52a}$$

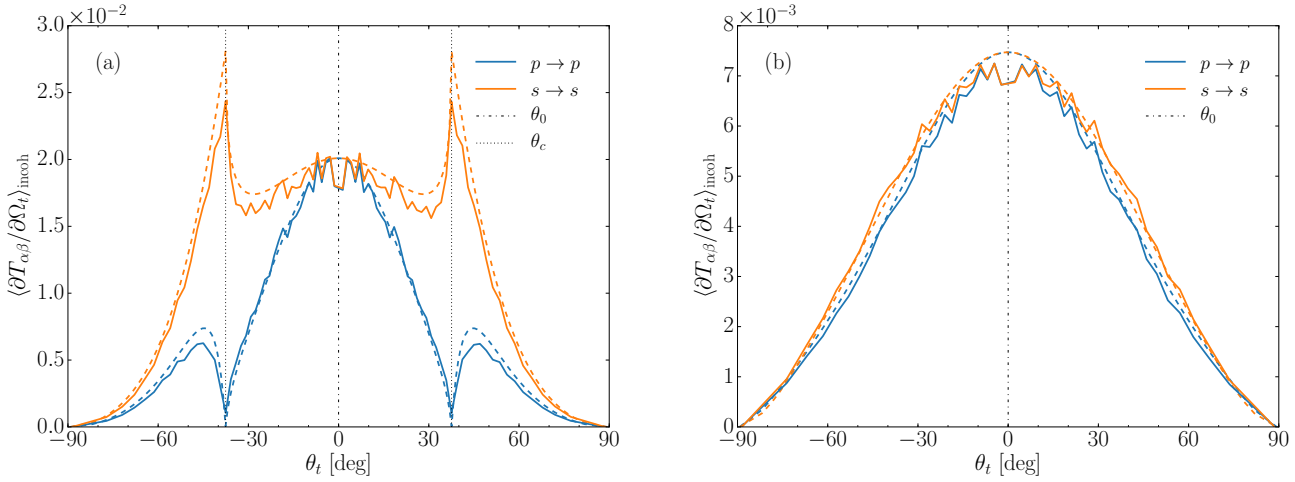

FIG. 2. The contribution to the incoherent component of the mean differential transmission coefficient from the in-plane, co-polarized transmission of p- and s-polarized light incident normally [$\theta_0 = 0°$] on the random vacuum-dielectric interface as a function of the angle of transmission θ_t. (a) The medium of incidence is vacuum [$\varepsilon_1 = 1$; $\varepsilon_2 = 2.6869$]; (b) The medium of incidence is the dielectric [$\varepsilon_1 = 2.6869$; $\varepsilon_2 = 1$]. Results for (in-plane) cross-polarized transmission have not been indicated since they are generally suppressed in the plane-of-incidence. The results presented as solid lines were obtained on the basis of numerically solving the reduced Rayleigh equation (26) for an ensemble of 7500 surface realizations. The dashed curves represent the result of the small amplitude perturbation theory (52) assuming polarization as indicated for the solid lines of the same color. The specular direction of transmission is indicated by the vertical dash-dotted line at $\theta_t = 0°$, and in Fig. 2(a), the vertical dotted lines at $\theta_t = \pm\theta_t^\star$ indicate the position of the critical angle where $\theta_t^\star = \arcsin(\sqrt{\varepsilon_1/\varepsilon_2}) \approx 37.5°$ for the parameters assumed. The wavelength of the incident light in vacuum was λ. The rough interface was assumed to have a root-mean-square roughness of $\delta = \lambda/20$, and it was characterized by an isotropic Gaussian power spectrum (3) of transverse correlation length $a = \lambda/4$. In the numerical calculations it was assumed that the surface covered an area $L \times L$, with $L = 25\lambda$, and the surface was discretized on a grid of 321×321 points. Add comment regarding the meaning of $\theta_t < 0$!

$$\left\langle \frac{\partial T_{ps}(\mathbf{q}_\parallel|\mathbf{k}_\parallel)}{\partial\Omega_t} \right\rangle_{\rm incoh} = \frac{\delta^2}{\pi^2}(\varepsilon_2-\varepsilon_1)^2 \frac{\varepsilon_2^{5/2}}{\varepsilon_1^{1/2}} \left(\frac{\omega}{c}\right)^4 \frac{\cos^2\theta_t}{\cos\theta_0} g(|\mathbf{q}_\parallel - \mathbf{k}_\parallel|) \frac{|\alpha_1(q_\parallel)|^2}{|d_p(q_\parallel)|^2} \left(\left[\hat{\mathbf{q}}_\parallel \times \hat{\mathbf{k}}_\parallel\right]_3 \right)^2 \frac{\alpha_1^2(k_\parallel)}{|d_s(k_\parallel)|^2} \tag{52b}$$

$$\left\langle \frac{\partial T_{sp}(\mathbf{q}_\parallel|\mathbf{k}_\parallel)}{\partial\Omega_t} \right\rangle_{\rm incoh} = \frac{\delta^2}{\pi^2}(\varepsilon_2-\varepsilon_1)^2 \frac{\varepsilon_2^{1/2}}{\varepsilon_1^{1/2}} \left(\frac{\omega}{c}\right)^4 \frac{\cos^2\theta_t}{\cos\theta_0} g(|\mathbf{q}_\parallel - \mathbf{k}_\parallel|) \frac{1}{|d_s(q_\parallel)|^2} \left(\left[\hat{\mathbf{q}}_\parallel \times \hat{\mathbf{k}}_\parallel\right]_3 \right)^2 \frac{\alpha_1^2(k_\parallel)\,|\alpha_2(k_\parallel)|^2}{|d_p(k_\parallel)|^2} \tag{52c}$$

$$\left\langle \frac{\partial T_{ss}(\mathbf{q}_\parallel|\mathbf{k}_\parallel)}{\partial\Omega_t} \right\rangle_{\rm incoh} = \frac{\delta^2}{\pi^2}(\varepsilon_2-\varepsilon_1)^2 \frac{\varepsilon_2^{3/2}}{\varepsilon_1^{1/2}} \left(\frac{\omega}{c}\right)^6 \frac{\cos^2\theta_t}{\cos\theta_0} g(|\mathbf{q}_\parallel - \mathbf{k}_\parallel|) \frac{1}{|d_s(q_\parallel)|^2} (\hat{\mathbf{q}}_\parallel \cdot \hat{\mathbf{k}}_\parallel)^2 \frac{\alpha_1^2(k_\parallel)}{|d_s(k_\parallel)|^2}, \tag{52d}$$

where the functions $d_\alpha(q_\parallel)$ and $d_\alpha(k_\parallel)$ for $\alpha = p, s$ are presented in Eq. (B11). Moreover, with the aid of $q_\parallel = \sqrt{\varepsilon_2}(\omega/c)\sin\theta_t$ the former of these functions can be written in the form

$$d_p(q_\parallel) = \sqrt{\varepsilon_2}\frac{\omega}{c}\left\{\varepsilon_2\left[\left(\frac{\varepsilon_1-\varepsilon_2}{\varepsilon_2}\right) + \cos^2\theta_t\right]^{\frac{1}{2}} + \varepsilon_1\cos\theta_t\right\} \tag{53a}$$

$$d_s(q_\parallel) = \sqrt{\varepsilon_2}\frac{\omega}{c}\left\{\left[\left(\frac{\varepsilon_1-\varepsilon_2}{\varepsilon_2}\right) + \cos^2\theta_t\right]^{\frac{1}{2}} + \cos\theta_t\right\}, \tag{53b}$$

and from $k_\parallel = \sqrt{\varepsilon_1}(\omega/c)\sin\theta_0$ the latter can be expresses as

$$d_p(k_\parallel) = \sqrt{\varepsilon_1}\frac{\omega}{c}\left\{\varepsilon_1\left[\left(\frac{\varepsilon_2-\varepsilon_1}{\varepsilon_1}\right) + \cos^2\theta_0\right]^{\frac{1}{2}} + \varepsilon_2\cos\theta_0\right\} \tag{53c}$$

$$d_s(k_\parallel) = \sqrt{\varepsilon_1}\frac{\omega}{c}\left\{\left[\left(\frac{\varepsilon_2-\varepsilon_1}{\varepsilon_1}\right) + \cos^2\theta_0\right]^{\frac{1}{2}} + \cos\theta_0\right\}. \tag{53d}$$

In applying Eq. (52) to the in-plane transmission whose results are depicted in Figs. 2(a) and 2(b) we set $\hat{\mathbf{q}}_\parallel \parallel \hat{\mathbf{k}}_\parallel$ [13].

We see from Eqs. (53a) and (53b) that when ε_1 is greater than ε_2, both $d_p(q_\parallel)$ and $d_s(q_\parallel)$ are real continuous monotonically decreasing functions of θ_t, and so therefore are $|d_p(q_\parallel)|^2$ and $|d_s(q_\parallel)|^2$. This leads to smooth dependencies of

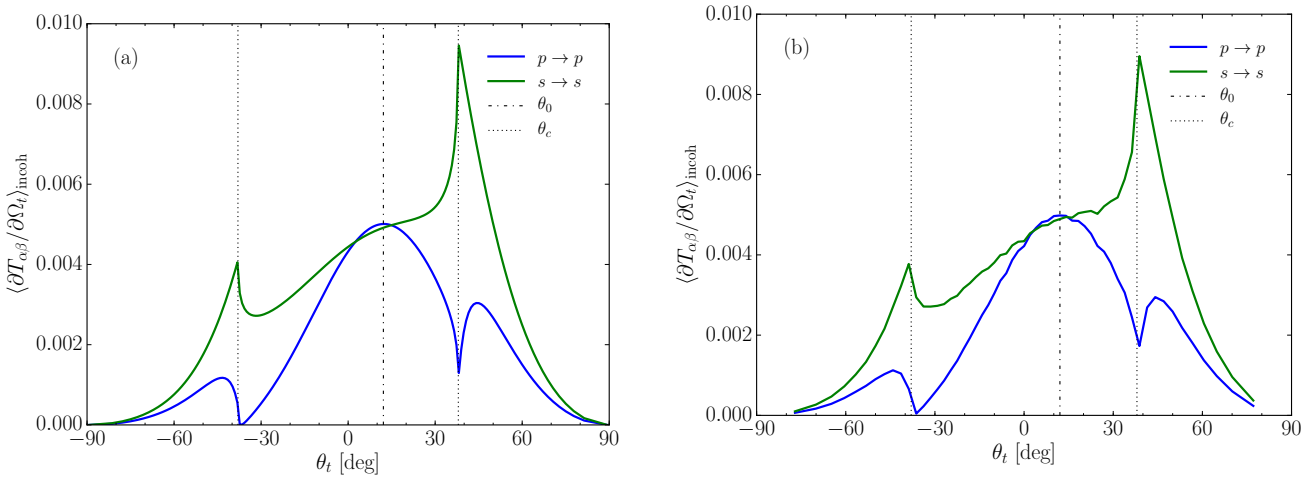

FIG. 3. The incoherent components of the mean differential transmission coefficients for in-plane, co-polarized transmission through a rough dielectric surface as functions of the polar angle of transmission, θ_t, as calculated by (a) perturbation theory, Eq. (52), and (b) the reduced Rayleigh equation (26). The media of incidence and transmission were vacuum and a dielectric, respectively [$\varepsilon_1 = 1$; $\varepsilon_2 = 2.6869$]. The polar angle of the incident light was $\theta_0 = 20^\circ$, which corresponds to a specular direction of transmission defined by the polar angle $\theta_t \approx 12.2^\circ$. The critical angle is still at $|\theta_t| = \theta_c = \arcsin(\sqrt{\varepsilon_1/\varepsilon_2})$. The values of other parameters are identical to those assumed in obtaining the results of Fig. 2.

the mean differential transmission coefficients on the angle of transmission [Fig. 2(b)]. However, when ε_a is less than ε_2, the first term in the expressions for $d_p(q_\parallel)$ and $d_s(q_\parallel)$ vanishes for a polar angle of transmission $\theta_t = \theta_t^\star$ defined by $\cos\theta_t^\star = [(\varepsilon_2 - \varepsilon_1)/\varepsilon_2]^{\frac{1}{2}}$, or, equivalently, when $\sin\theta_t^\star = \sqrt{\varepsilon_1/\varepsilon_2}$, and becomes pure imaginary as θ_t increases beyond the angle

$$\theta_t^\star = \arcsin\sqrt{\frac{\varepsilon_1}{\varepsilon_2}}. \tag{54}$$

The functions $|d_p(q_\parallel)|^{-2}$ and $|d_s(q_\parallel)|^{-2}$ therefore display asymmetric peaks at the polar angle of transmission $\theta_t = \theta_t^\star$. These are the optical analogues of the *Yoneda peaks* observed in the scattering of x-rays from a metal surface [6, 7]. The results of a numerical evaluation of Eqs. (52a) and (52d) are depicted as dashed lines in Fig. 2. From this figure it is observed that the single-scattering perturbation theory reproduces fairly well the overall shape of the mean differential transmission coefficients for in-plane co-polarized transmission, at least for the level of roughness assumed in producing these results. However, there seems to be some minor difference in amplitude between the simulations results and the curves produced from perturbation theory, in particular when $\varepsilon_1 < \varepsilon_2$.

There is a second feature of Eq. (52a) that deserves a comment. The function $\alpha_1(q_\parallel)\alpha_2(k_\parallel) + q_\parallel k_\parallel$ that appears in the numerator on the right-hand side of this equation can, when $\mathbf{q}_\parallel \parallel \mathbf{k}_\parallel$, be written explicitly in the form (CHECK!)

$$\alpha_1(q_\parallel)\alpha_2(k_\parallel) + q_\parallel k_\parallel = \sqrt{\varepsilon_1\varepsilon_2}\left(\frac{\omega}{c}\right)^2 \left\{ \left[\frac{\varepsilon_1}{\varepsilon_2} - \sin^2\theta_t\right]^{\frac{1}{2}} \left[\frac{\varepsilon_2}{\varepsilon_1} - \sin^2\theta_0\right]^{\frac{1}{2}} + \sin\theta_t \sin\theta_0 \right\}. \tag{55}$$

Considered as a function of θ_t for a fixed value of θ_0, we see that when $\varepsilon_1 > \varepsilon_2$ this function is structureless, and its squared modulus introduces no feature into $\langle \partial T_{pp}(\mathbf{q}_\parallel|\mathbf{k}_\parallel)/\partial\Omega_t \rangle_{\rm incoh}$. However, when $\varepsilon_1 < \varepsilon_2$ the factor $[\varepsilon_1/\varepsilon_2 - \sin^2\theta_t]^{1/2}$ is real and decreases with increasing θ_t in the interval $0 < \theta_t < \theta_t^\star$; it vanishes at $\theta_t = \theta_t^\star$; and is pure imaginary and increases in magnitude with increasing θ_t in the interval $\theta_t^\star < \theta_t < \pi/2$. Consequently the squared modulus of the expression given by Eq. (55) possesses an asymmetric minimum at $\theta_t = \theta_t^\star$, and so therefore does $\langle \partial T_{pp}(\mathbf{q}_\parallel|\mathbf{k}_\parallel)/\partial\Omega_t \rangle_{\rm incoh}$. This feature is readily observed in Fig. 2(a).

Because the Yoneda peaks and the minimum are present in the expressions for the mean differential transmission coefficient obtained in the lowest order in the surface profile function, the second, they are single-scattering phenomena, not multiple-scattering effects. This is confirmed by the qualitative similarity between the plots in Figs. 3(a) and 3(b). It should also be noted that the polar angle of transmission where the Yoneda phenomenon can be observed is determined only by the ratio of the dielectric constants of the two media; it does not, for instance, depend on the angles of incidence [see Figs. 2 and 3].

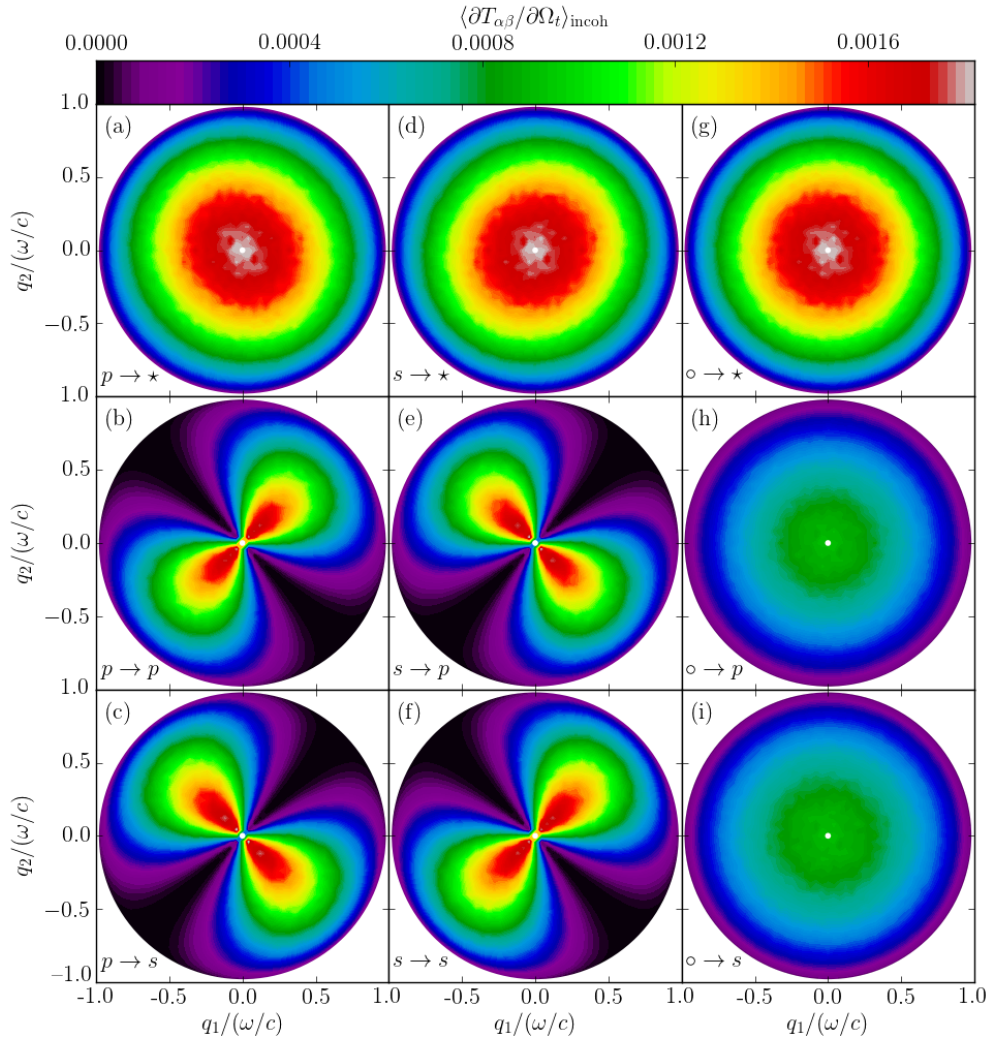

FIG. 4. The incoherent component of the mean differential transmission coefficient, showing the full angular intensity distribution as a function of the lateral wavevector of the light transmitted from a dielectric medium into vacuum separated by a rough interface. The angles of incidence were $(\theta_0, \phi_0) = (0^\circ, 45^\circ)$. The position of the specular direction in transmission is indicated by white dots. The parameters assumed for the scattering geometry and used in performing the numerical simulations had values that are identical to those assumed in obtaining the results of Fig. 2(a). The in-plane intensity variations in Figs. 4(b) and 4(f) are the curves depicted in Fig. 2(a). The star notation, *e.g.* $p \to \star$, indicates that the polarization of the transmitted light was not recorded. Furthermore, in *e.g* Fig. 4(g), the open circle in $\circ \to \star$ symbolizes that the incident light was unpolarized; this simulation result was obtained by adding *half* of the results from Figs. 4(a) and 4(d).

We now turn to the angular intensity distributions of the transmitted light. In Figs. 4 and 5 we present simulation results for the contribution to the mean differential transmission coefficient from the light that has been transmitted incoherently through the randomly rough interface, that display the full angular distribution of this contribution. These two figures were obtained under the assumption that the angles of incidence were $(\theta_0, \phi_0) = (0^\circ, 45^\circ)$; it was cuts along the plane of incidence of these angular intensity distributions that resulted in the curves presented in Fig. 2. Therefore, the parameters assumed in producing the results of Figs. 2(a) and 4 are identical, and so are the parameters assumed in obtaining Figs. 2(b) and 5.

All angular intensity distributions that we present in this work, including those in Figs. 4 and 5, are organized in the same fashion. They are arranged in 3×3 subfigures where each row and column of the array correspond to the angular distribution of the incoherent component of the mean differential transmission coefficient for a given state of polarization of the transmitted and incident light, respectively. The lower left 2×2 corner of such figures corresponds to the cases where β-polarized incident light is transmitted by the rough interface into α-polarized light,

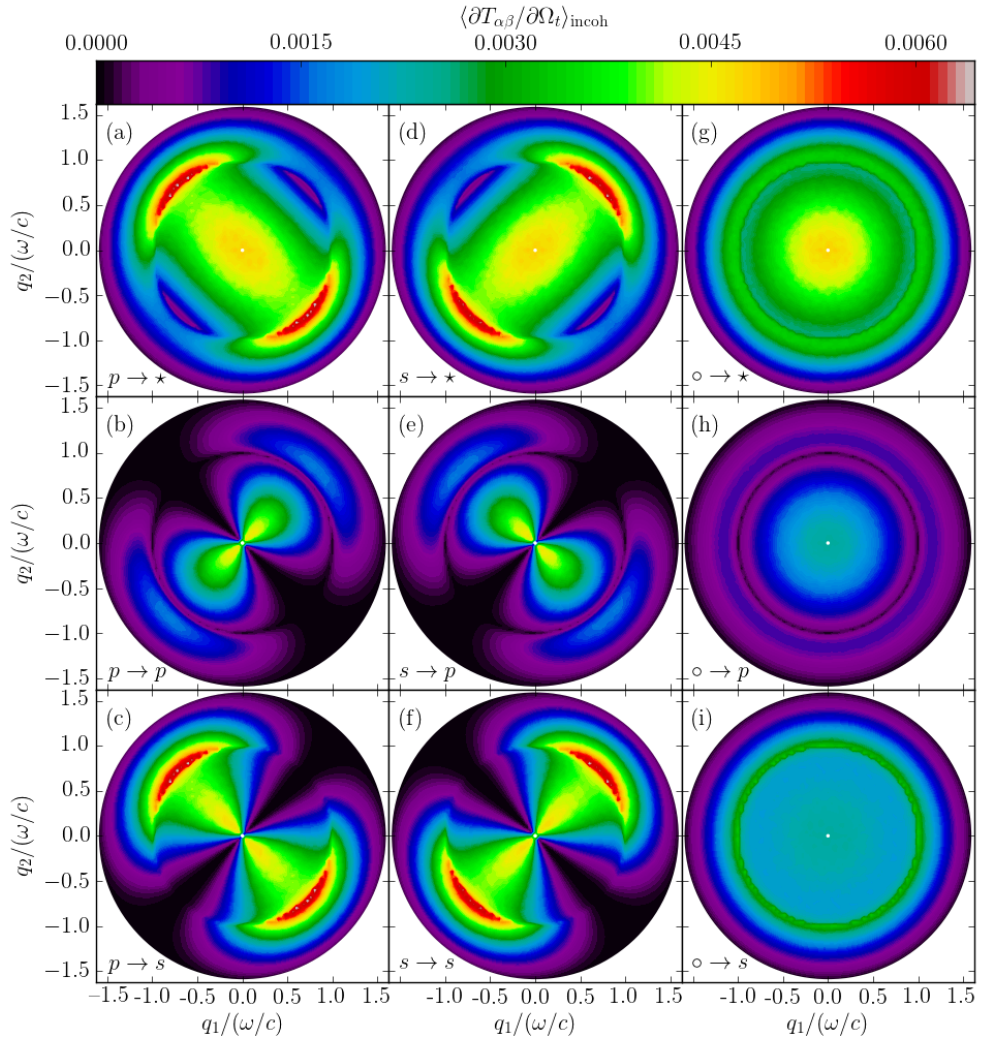

FIG. 5. The same as Fig. 4, but for light incident from the vacuum side onto the dielectric. Notice the rapid changes in intensity around the polar angle $\theta_t = \theta_c = \arcsin(\sqrt{\varepsilon_1/\varepsilon_2})$. The in-plane intensity variations in Figs. 5(b) and 5(f) are the curves depicted in Fig. 2(b).

denoted $\beta \to \alpha$ in the lower left corner of each subfigure, where $\alpha = p, s$ and the same for β. Moreover, the first row corresponds to results where the polarization of the transmitted light was not recorded (indicated by $\star$); such results are obtained by adding the other two results from the same column. The last column of the angular intensity distribution figures corresponds to the situation when the incident light is *unpolarized* (indicated by an open circle, $\circ$); these results are obtained by adding *half* of the other two results present in the same row. For instance, the subfigure in the upper right corner, labeled $\circ \to \star$, refers to unpolarized light (the open circle) transmitted by the surface into light for which we do not record the polarization (the star). It should be stressed that even if the polarization of the transmitted light is not recorded, it does not mean that the transmitted light is unpolarized; in general this is not the case as can be seen by, for instance, inspecting Fig. 5.

When both the incident and transmitted light are linearly polarized, the lower left 2×2 corners of Figs. 4 and 5 show that the angular distributions of the incoherent component of the mean differential transmission coefficients take on dipole-like patterns oriented along the plane-of-incidence for co-polarization and perpendicular to it for cross-polarization. We note that such patterns are a consequence of our definition used for the polarization vectors, and that similar patterns have recently been observed in reflection [2, 14]. It was already concluded based on Fig. 2 that the in-plane, co-polarized transmission is rather different for p and s polarization when the medium of incidence is vacuum, and rather similar when the medium of incidence is the dielectric. Not surprisingly, a similar conclusion can be drawn by inspecting the co-polarized angular intensity distributions depicted in the $\beta \to \beta$ subfigures of Figs. 4

and 5 [$\beta = p, s$]. For normal incidence, the angular intensity distributions for cross- and co-polarized transmission are intimately related to each other, but only if they share the same polarization state of the transmitted light; in fact, the former distributions are 45° rotations of the latter. For instance for scattering into s-polarized light, this can be understood if we note from Eqs. (52c), (52d) and (27) [see also Eq. (B13) of Appendix B] that to the lowest nonzero order in $\zeta(\mathbf{x}_\parallel)$ we have

$$\left\langle \frac{\partial T_{sp}(\mathbf{q}_\parallel|\mathbf{k}_\parallel)}{\partial\Omega_t} \right\rangle_{\text{incoh}} = \frac{\delta^2}{\pi^2}(\varepsilon_2-\varepsilon_1)^2\varepsilon_1^{1/2}\varepsilon_2^{5/2}\left(\frac{\omega}{c}\right)^2\frac{\cos^2\theta_t}{\cos\theta_0}g(|\mathbf{q}_\parallel-\mathbf{k}_\parallel|)\frac{\left|M_{sp}(\mathbf{q}_\parallel|\mathbf{k}_\parallel)\right|^2\alpha_1^2(k_\parallel)}{|d_s(q_\parallel)|^2|d_p(k_\parallel)|^2} \tag{56a}$$

$$\left\langle \frac{\partial T_{ss}(\mathbf{q}_\parallel|\mathbf{k}_\parallel)}{\partial\Omega_t} \right\rangle_{\text{incoh}} = \frac{\delta^2}{\pi^2}(\varepsilon_2-\varepsilon_1)^2\frac{\varepsilon_2^{3/2}}{\varepsilon_1^{1/2}}\left(\frac{\omega}{c}\right)^2\frac{\cos^2\theta_t}{\cos\theta_0}g(|\mathbf{q}_\parallel-\mathbf{k}_\parallel|)\frac{\left|M_{ss}(\mathbf{q}_\parallel|\mathbf{k}_\parallel)\right|^2\alpha_1^2(k_\parallel)}{|d_s(q_\parallel)|^2|d_s(k_\parallel)|^2}, \tag{56b}$$

where the matrix elements $M_{sp}(\mathbf{q}_\parallel|\mathbf{k}_\parallel)$ and $M_{ss}(\mathbf{q}_\parallel|\mathbf{k}_\parallel)$ are presented in Eq. (27). For normal incidence, $d_p(0)/\sqrt{\varepsilon_1\varepsilon_2} = d_s(0)$ and $M_{sp}(\mathbf{q}_\parallel|\mathbf{0})$ out-of-plane equals $M_{ss}(\mathbf{q}_\parallel|\mathbf{0})$ in-plane. This means that $\langle\partial T_{sp}(\mathbf{q}_\parallel|\mathbf{0})/\partial\Omega_t\rangle_{\text{incoh}}$ will equal $\langle\partial T_{ss}(\mathbf{q}'_\parallel|\mathbf{0})/\partial\Omega_t\rangle_{\text{incoh}}$ if $\mathbf{q}_\parallel$, after a rotation by an angle of 45°, equals $\mathbf{q}'_\parallel$. A similar argument can be used to relate the angular distribution of $\langle\partial T_{ps}(\mathbf{q}_\parallel|\mathbf{0})/\partial\Omega_t\rangle_{\text{incoh}}$ after a 45° rotation of the angular distribution of $\langle\partial T_{pp}(\mathbf{q}_\parallel|\mathbf{0})/\partial\Omega_t\rangle_{\text{incoh}}$. This symmetry property of the angular intensity distributions at normal incidence is readily observed in Figs. 4 and 5. Hence, we conclude that the regions of high intensity observed in the cross-polarized angular intensity distribution in Fig. 5(c) around the out-of-plane direction are also Yoneda peaks; their origin is due to the peaking factor $|d_s(q_\parallel)|^{-2}$ vs. transmitted wave-number, just like we found for the in-plane peaks in the co-polarized transmitted light.

When $\varepsilon_1 < \varepsilon_2$, Yoneda peaks may actually be observed for a wide range of azimuthal angles of transmission. For instance, at normal incidence, and when unpolarized incident light is transmitted through the surface into s-polarized light, the Yoneda peaks occur around $\theta_t = \theta_c$ [or $q_\parallel = \sqrt{\varepsilon_1}\omega/c$] independent of the value of the azimuthal angle of transmission ϕ_t, and they will have constant height [Fig. 5(i)]. Similarly, when unpolarized light is transmitted into p-polarized light for the same scattering system, one observes from Fig. 5(h) that a circular grove exist at $q_\parallel = \sqrt{\varepsilon_1}\omega/c$. For normal incidence [$k_\parallel = 0$], the amplitudes of $\langle\partial T_{pp}(\mathbf{q}_\parallel|\mathbf{k}_\parallel)/\partial\Omega_t\rangle_{\text{incoh}}$ and $\langle\partial T_{ps}(\mathbf{q}_\parallel|\mathbf{k}_\parallel)/\partial\Omega_t\rangle_{\text{incoh}}$ at the position of the groove will be zero according to (52a) and (52b). This is due to the factor $\alpha_1(q_\parallel)$, since it vanishes when $q_\parallel = \sqrt{\varepsilon_1}\omega/c$.

It should be observed from Figs. 4(g)–(i) and 5(g)–(i), that at normal incidence, and due to the isotropy of the surface, unpolarized incident light will be transmitted by the surface into rotationally symmetric intensity distributions independent of whether the transmitted light is p- or s-polarized. When unpolarized light is incident from the dielectric, there are only minor differences in the intensity distributions of the p- and s-polarized transmitted light [Figs. 4(h)–(i)]. However, when the light is incident from vacuum, Figs. 5(h)–(i) show pronounced differences in their intensity distributions.

B. Non-normal incidence

We now address the situation when $\theta_0 \neq 0°$, and we start our discussion by assuming that the light is incident from the dielectric onto the rough interface. Figures 6 and 7 present the full angular distributions of the transmitted intensities for angles of incidence $(\theta_0, \phi_0) = (20°, 45°)$ and $(\theta_0, \phi_0) = (64°, 45°)$, respectively. The main feature we observe from these figures is that as the polar angle of incidence is increased from zero, the incident light is transmitted more-and-more into the forward transmission plane. The distributions in Figs. 6 and 7 are rather smooth with few, if any, surprising characteristics. It should be noted that the polar angle of incidence $\theta_0 = 64°$ is larger than the critical angle for total internal reflection, $\theta_c = \arcsin(\sqrt{\varepsilon_2/\varepsilon_1}) \approx 38.0°$, so, for the equivalent planar system, no light should have been transmitted at all; the nonzero intensity distributions observed in Fig. 7 are therefore all roughness induced.

It is now assumed that the light is incident from vacuum. In Figs. 8 and 9 the mean differential transmission coefficients for light that has been transmitted incoherently by the surface are presented for angles of incidence $(\theta_0, \phi_0) = (20°, 45°)$ and $(\theta_0, \phi_0) = (64°, 45°)$, respectively. The observation made for the dielectric-vacuum system that an increase in θ_0 will result in the majority of the light being transmitted into the forward transmission plane, is also true for the vacuum-dielectric system. However, Figs. 8 and 9 show several characteristic features, of which the Yoneda peaks located at $q_\parallel = \sqrt{\varepsilon_1}\omega/c$ are the most prominent.

In the case of $\theta_0 = 20°$, Fig. 8 shows that the Yoneda peaks are still prominent, but their amplitudes are no longer independent of the azimuthal angle of transmission, as was found for normal incidence. For $s \to s$ transmission, Fig. 8(f), it is found that the Yoneda peak amplitudes are higher in the forward transmission plane than in the backward plane, and the former peaks have a higher amplitude than they had for normal incidence. Moreover, the Yoneda peaks visible in cross-polarized $p \to s$ transmission, Fig. 8(c), that for normal incidence were located symmetrically

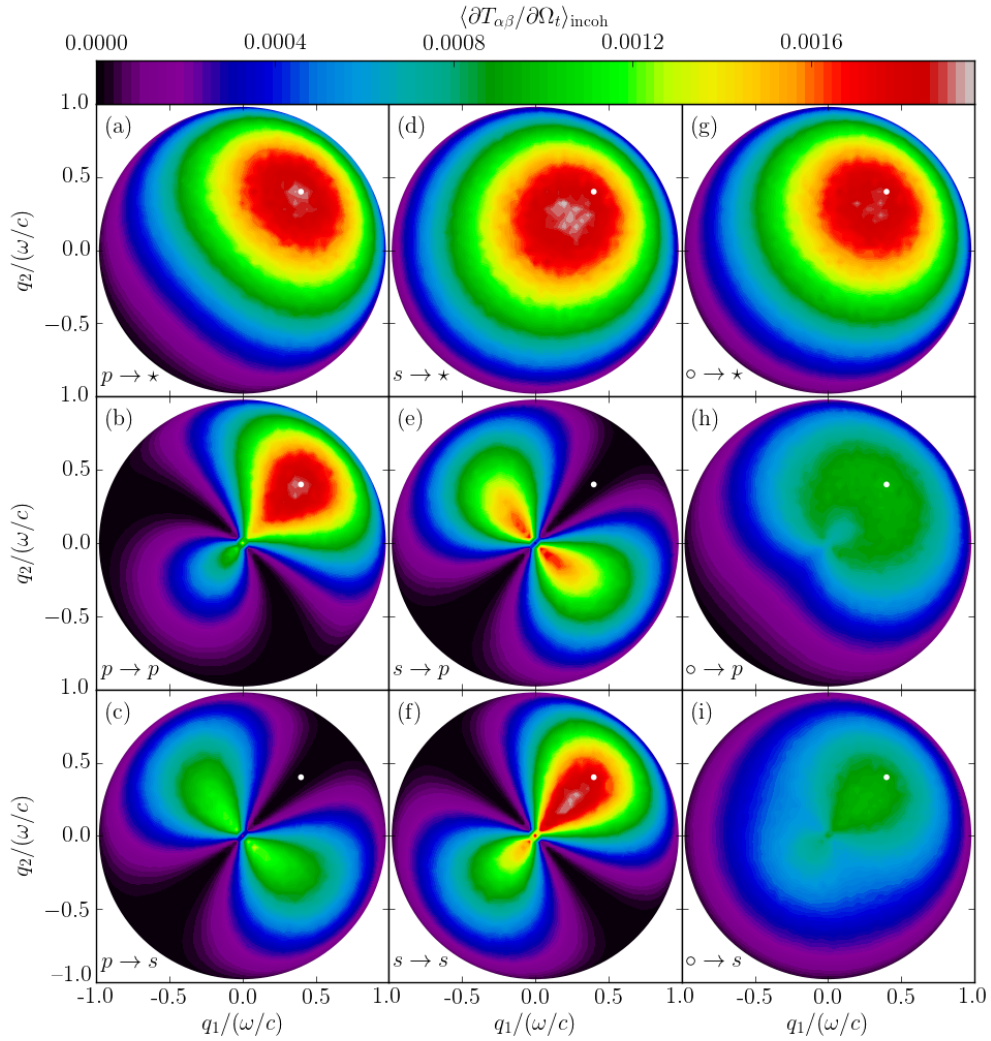

FIG. 6. Same as Fig. 4, but for the angles of incidence $(\theta_0, \phi_0) = (20^\circ, 45^\circ)$.

out-of-plane, are now moving into the forward transmission plane. The amplitude of $\langle \partial T_{p\alpha}(\mathbf{q}_\parallel|\mathbf{k}_\parallel)/\partial\Omega_t \rangle_{\rm incoh}$ when $q_\parallel = \sqrt{\varepsilon_1}\omega/c$, which was essentially zero for normal incidence, does no longer vanish everywhere as can be seen in the second row of subfigures in Fig. 8. We still observe a local minimum in the transmitted intensity into p-polarized light at the position of the Yoneda peaks and this intensity is, in the plane of incidence, substantially lower than the corresponding intensity for transmission into s-polarized light.

However, when the polar angle of incidence is increased to $\theta_0 = 64^\circ$, Fig. 9 shows that p-polarized transmitted light gives a significant, maybe even dominant, contribution to in-plane transmitted intensity at the position of the Yoneda peak in the forward transmission plane [$\phi_t = \phi_0$]. This is in sharp contrast to what was found when $\theta_0 = 0^\circ$ and $\theta_0 = 20^\circ$, where s-polarized transmitted light gave the most significant contribution to the in-plane transmitted intensity at the position of the Yoneda peaks. To explain this behavior, we will again be assisted by Eq. (52a), from which it follows that at the position of the Yoneda peaks

$$\left\langle \frac{\partial T_{pp}(\mathbf{q}_\parallel|\mathbf{k}_\parallel)}{\partial\Omega_t} \right\rangle_{\rm incoh}\Bigg|_{q_\parallel=\sqrt{\varepsilon_1}\omega/c} \propto \frac{k_\parallel^2}{\left|d_p(k_\parallel)\right|^2}, \tag{57}$$

where we used $\alpha_1(\sqrt{\varepsilon_1}\omega/c) = 0$ in obtaining this result. For normal incidence, Eq. (57) predicts that the $p \to p$ transmission should go to zero, consistent with what we have seen. However, as the polar angle of incidence is increased, the function on the right-hand-side of Eq. (57) will grow quickly, particularly as one approaches grazing incidence. This has the consequence that $\langle \partial T_{pp}(\mathbf{q}_\parallel|\mathbf{k}_\parallel)/\partial\Omega_t \rangle_{\rm incoh}$, for increasing polar angle of incidence, will go from

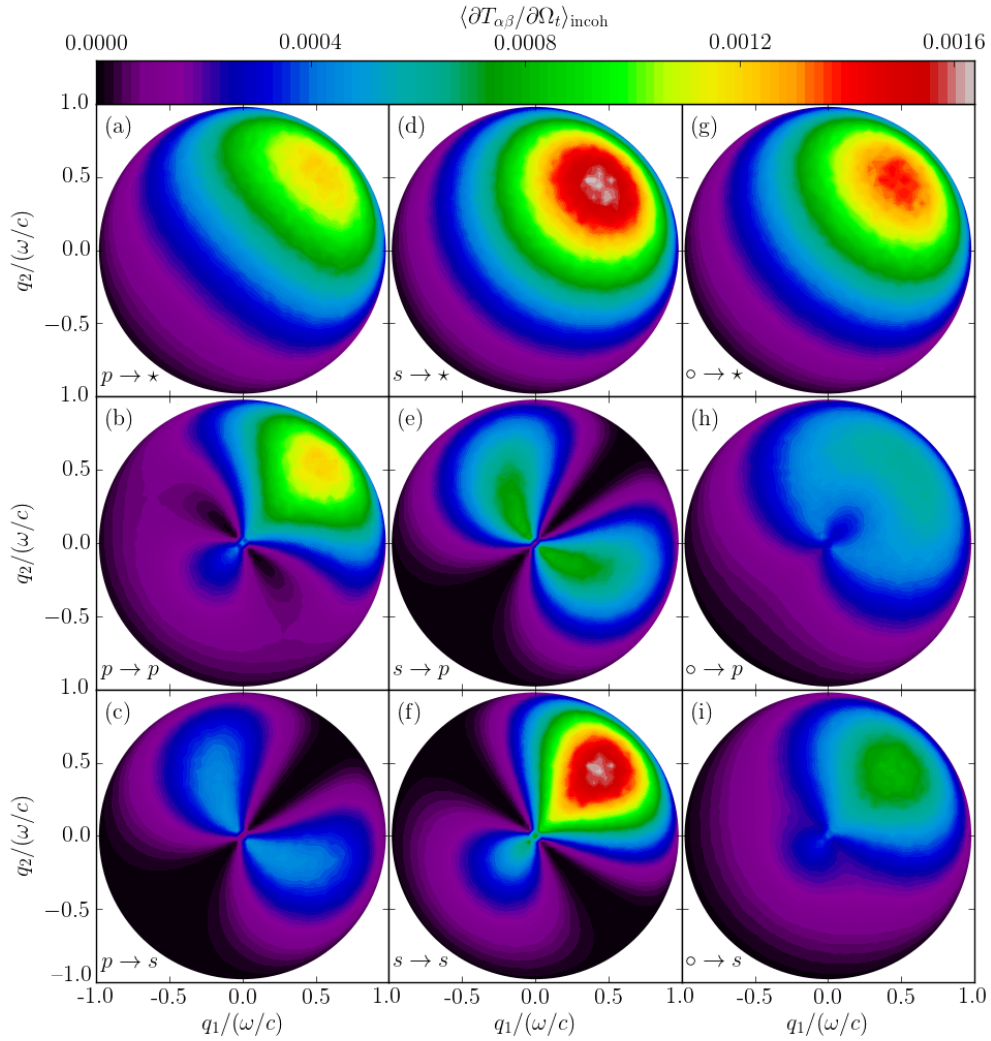

FIG. 7. Same as Fig. 4, but for the angles of incidence $(\theta_0, \phi_0) = (64°, 45°)$. Note that for a corresponding flat interface system, there would have been zero transmission, since the incident field will experience total internal reflection due to $\theta_0 > \theta_c \approx 38.0°$. For this reason there is no white dot indicating the specular direction of transmission in this case. For this rough interface system, the light that is transmitted is induced by the surface roughness.

dipping to peaking at the position of the Yoneda peaks, $q_\parallel = \sqrt{\varepsilon_1}\omega/c$. This will not happen for the $s \to p$ transmitted light since to lowest order in the surface profile function its intensity is proportional to $\alpha_1(q_\parallel)$, which will always be zero at the position of the Yoneda peaks [see Eq. (52c)].

To illustrate this behavior, we study the co-polarized transmitted intensity at the position of the Yoneda peak in the forward transmission plane, $(\theta_t, \phi_t) = (\theta_c, \phi_0)$, by defining the quantity

$$Y_\alpha(\theta_0) \equiv \left\langle \frac{\partial T_{\alpha\alpha}(\mathbf{q}_\parallel|\mathbf{k}_\parallel)}{\partial\Omega_t} \right\rangle_{\rm incoh} \Bigg|_{\mathbf{q}_\parallel = \sqrt{\varepsilon_1}\frac{\omega}{c}\hat{\mathbf{k}}_\parallel}. \tag{58}$$

Figure 10 presents simulation results for $Y_\alpha(\theta_0)$ as a function of polar angle of incidence for the transmission through the vacuum-dielectric system. This figure shows, as is consistent with the above discussion, that $Y_p(\theta_0)$ increases more rapidly than $Y_s(\theta_0)$ for moderate angles of incidence; moreover, for an angle of incidence of about 62° and above, we find that $Y_p(\theta_0) \geq Y_s(\theta_0)$ for the dielectric constants assumed in the current work. Part of the reason that $Y_p(\theta_0 = 0°)$ is not quite zero, is that the simulation results assumes a polar angle of transmission that is slightly larger than the critical angle. Another reason for the nonzero $Y_p(\theta_0 = 0°)$ is multiple scattering effects which were included consistently in the non-perturbative simulation technique used to obtain the results of Fig. 10.

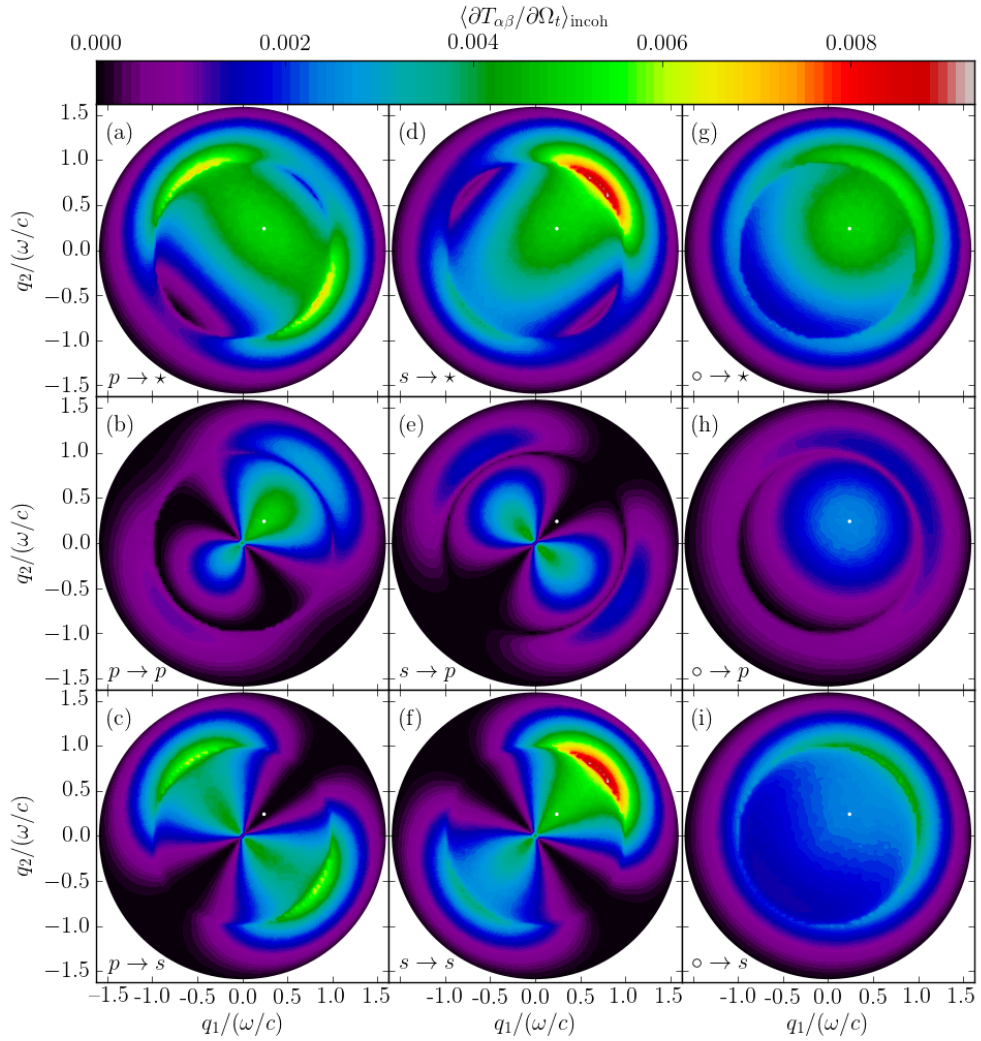

FIG. 8. Same as Fig. 5, but for the angles of incidence $(\theta_0, \phi_0) = (20°, 45°)$.

It should to be mentioned that the results presented in Figs. 4–9 are similar in many respects to those obtained in other recent numerical studies of related scattering geometries, in both reflection and transmission. A non-exhaustive selection of these includes light scattering in reflection from potentially strongly rough perfectly conduction surfaces [15, 16]; penetrable rough surfaces of, in principle any degree of roughness [12, 16, 17]; and weakly rough surfaces that are part of a simple surface or film geometry [2, 18, 19].

C. Transmissivity and transmittance

Apply the substitution $\theta_c \to \theta_c'$ in Fig. 11 and 12 and make sure it is used consistently throughout this section (but NOt in previous sections); Btw is this angle defined in these figure captions.

Turning now to the transmissivity (48) of the randomly rough interface, we present in Fig. 11(a) the transmissivity as a function of the polar angle of incidence θ_0 when the interface is illuminated from the dielectric by p- and s-polarized light. The transmissivity when the interface is illuminated from vacuum is presented in Fig. 11(b). The vanishing of the transmissivity for incident light of both polarizations for angles of incidence greater than the critical angle for total internal reflection, $\theta_c' = \arcsin(\sqrt{\varepsilon_2/\varepsilon_1})$ which evaluates to $\theta_c' = 38.0°$ for the assumed values of the dielectric constants, is clearly seen in Fig. 11(a). In contrast, in Fig. 11(b), the transmissivity for incident light of both polarizations is nonzero for all values of θ_0, and tends to zero at a grazing angle of incidence $\theta_0 \approx 90°$. The transmissivity is larger for p-polarized light than it is for s-polarized light, irrespective of the medium of incidence.

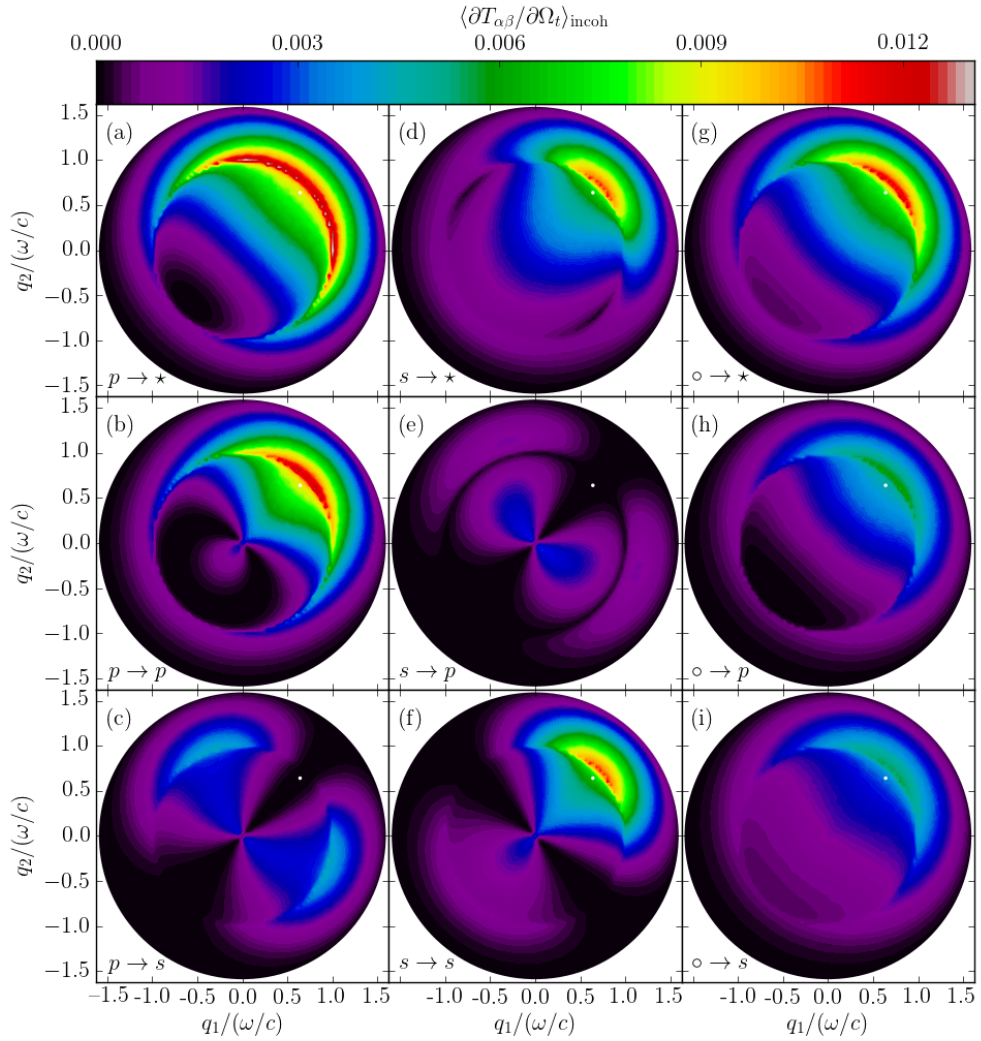

FIG. 9. Same as Fig. 5, but for the angles of incidence $(\theta_0, \phi_0) = (64°, 45°)$.

This is consistent with the result that the reflectivity of a dielectric surface is larger for s-polarized light than for p-polarized light [**?**]. Even if the transmissivity curves presented in Fig. 11 closely resemble the functional form of the transmissivity obtained for equivalent flat interface systems (the Fresnel transmission coefficients), we remark that there are differences, as quantified by the dashed lines in Fig. 11. For instance, from Fig. 11 one observes that $\mathscr{T}_p(\theta_0) < 1$ for all angles of incidence, while for the equivalent flat interface systems the transmissivity will be unity at the Brewster angle [] located around the maxima of $\mathscr{T}_p(\theta_0)$ in Fig. 11. (Find suitable references.)

We now focus on the contribution to the transmittance from the light that has been transmitted incoherently through the surface; in Eq. (51), this is the last term denoted $\mathscr{T}_\beta(\theta_0)_{\rm incoh}$ for incident light of β polarization. Figure 12(a) presents the transmittance $\mathscr{T}_\beta(\theta_0)_{\rm incoh}$ as a function of the polar angle of incidence when the incident medium is the dielectric, and it is found that this quantity displays interesting features. For instance, in s polarization, a sharp maximum is observed for an angle of incidence a little less than 40°, and for this angle of incidence, the contribution to the transmittance from the light being transmitted incoherently is about twice the value at normal incidence. This behavior one can understand in terms of Eq. (52d). As a function of incidence (or $k_\parallel$), the expression for $\langle \partial T_{ss}(\mathbf{q}_\parallel|\mathbf{k}_\parallel)/\partial\Omega_t \rangle_{\rm incoh}$ in this equation will have a maximum when $|d_s(k_\parallel)|^{-2}$ is peaking. This happens when $k_\parallel = \sqrt{\varepsilon_2}\omega/c$, or when $\theta_0 = \theta_c'$. The expression for the $s \to p$ transmission will also go through a maximum at the same critical angle [see Eq. (52b)], and so will therefore also $\mathscr{T}_s(\theta_0)_{\rm incoh}$. This explains the functional dependence of $\mathscr{T}_s(\theta_0)_{\rm incoh}$ on the angle of incidence. From Fig. 12(a) it is also observed that the two curves behave differently around $\theta_0 = \theta_c'$. While the transmittance $\mathscr{T}_s(\theta_0)_{\rm incoh}$ is monotonously increasing in the interval $0° < \theta_0 < \theta_c'$ and monotonously decreasing in the interval $\theta_c' < \theta_0 < 90°$, this is not the case for the transmittance of p-polarized

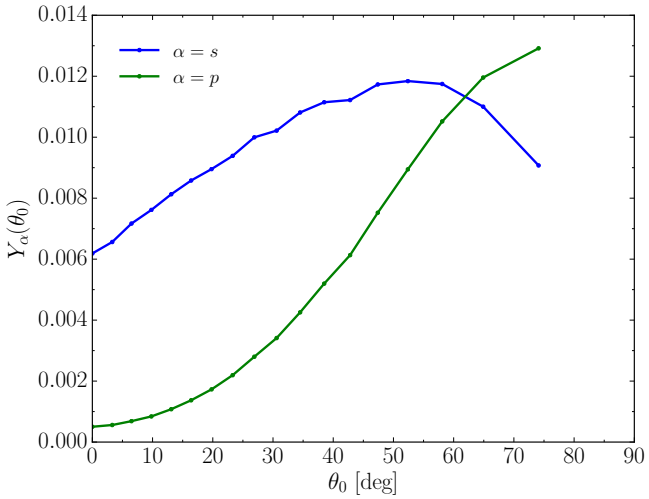

FIG. 10. Simulation results for the in-plane, co-polarized contribution to the transmission close to the Yoneda peak in the forward transmission plane as measured by the function $Y_\alpha(\theta_0)$ defined in Eq. (58). The simulation results are reported for $\theta_t = 38.8^\circ$ and $\phi_t = \phi_0 = 45^\circ$ where the former angle is slightly larger, due to the computational grid used, than the polar angle $\theta_t = \theta_c = 38.0^\circ$ where Yoneda peaks are expected.

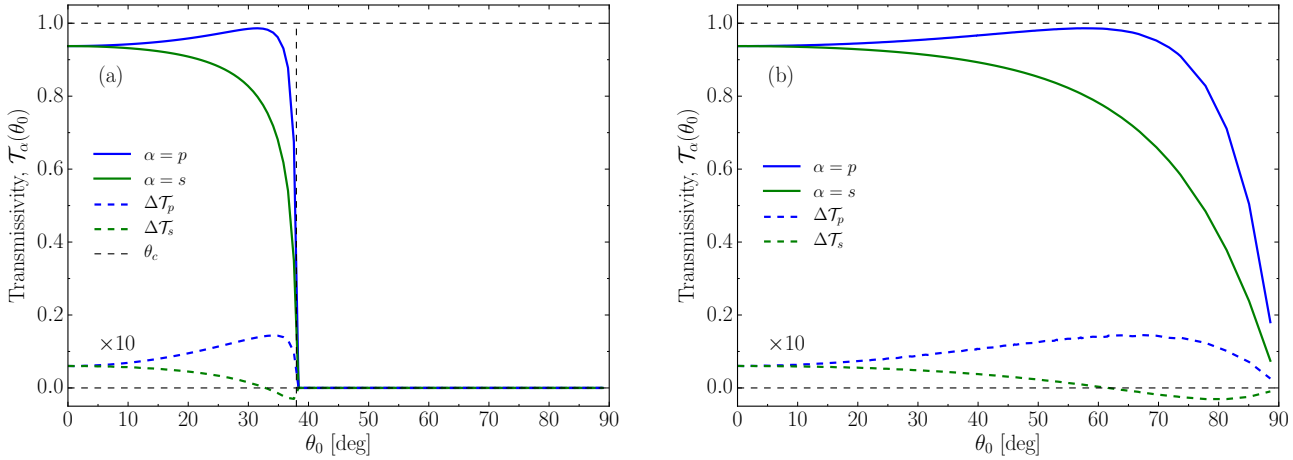

FIG. 11. (a) The transmissivities $\mathcal{T}_\alpha(\theta_0)$ of a two-dimensional randomly rough dielectric-vacuum interface ($\varepsilon_1 = 2.6869$, $\varepsilon_2 = 1$) for p- and s-polarized light as functions of the polar angle of incidence. (b) The same as in 11(a), but for a vacuum-dielectric interface ($\varepsilon_1 = 1$, $\varepsilon_2 = 2.6869$). The quantity $\Delta\mathcal{T}_\alpha(\theta_0) = \mathcal{T}_\alpha^F(\theta_0) - \mathcal{T}_\alpha(\theta_0)$ signifies the difference between the Fresnel transmission coefficient (flat surface transmissivity), $\mathcal{T}_\alpha^F(\theta_0)$, and the transmissivity for the equivalent rough interface scattering system. Ten times $\Delta\mathcal{T}_p(\theta_0)$ and $\Delta\mathcal{T}_s(\theta_0)$ are presented as dashed lines, and for most angles of incidence, these differences are positive. The critical angle $\theta_0 = \theta_c'$ for total internal reflection for the planar dielectric-vacuum system is indicated by the vertical dashed line; with the values assumed for the dielectric constants $\theta_c' \approx 38.0^\circ$. The roughness parameters assumed in obtaining these results are the same as in Fig. 2. Several simulations were run with small perturbations in the surface length L in order to obtain transmissivity data with higher angular resolution.

incident light. Similar to the case of s-polarized incident light, the rapid dependence on the angle of incidence of $\mathscr{T}_p(\theta_0)_{\rm incoh}$ around $\theta_0 = \theta_c'$ is due to the factor $|d_p(k_\parallel)|^{-2}$ present in Eqs. (52a) and Eq. (52c). However, unlike in the case of s-polarized incident light, the cross-polarized transmission, $\langle \partial T_{sp}(\mathbf{q}_\parallel|\mathbf{k}_\parallel)/\partial\Omega_t\rangle_{\rm incoh}$, Eq. (52c), will go to zero at the critical angle $\theta_0 = \theta_c'$ due to the factor $\alpha_2(k_\parallel)$ that is present in the expression for it. Therefore, for p-polarized incident light, the transmittance will have a contribution from co-polarized transmission which peaks at the critical angle of incidence, and a contribution from cross-polarization that has a dip down to zero at the critical angle, and it is the sum of the two that results in the functional form observed in Fig. 12(a).

The transmittance from vacuum into the dielectric is depicted in Fig. 12(b). In this situation for which $\varepsilon_1 < \varepsilon_2$, the functions $|d_p(k_\parallel)|^{-2}$ and $|d_s(k_\parallel)|^{-2}$ are both monotonously increasing functions of $k_\parallel$ (or θ_0), and the transmittances

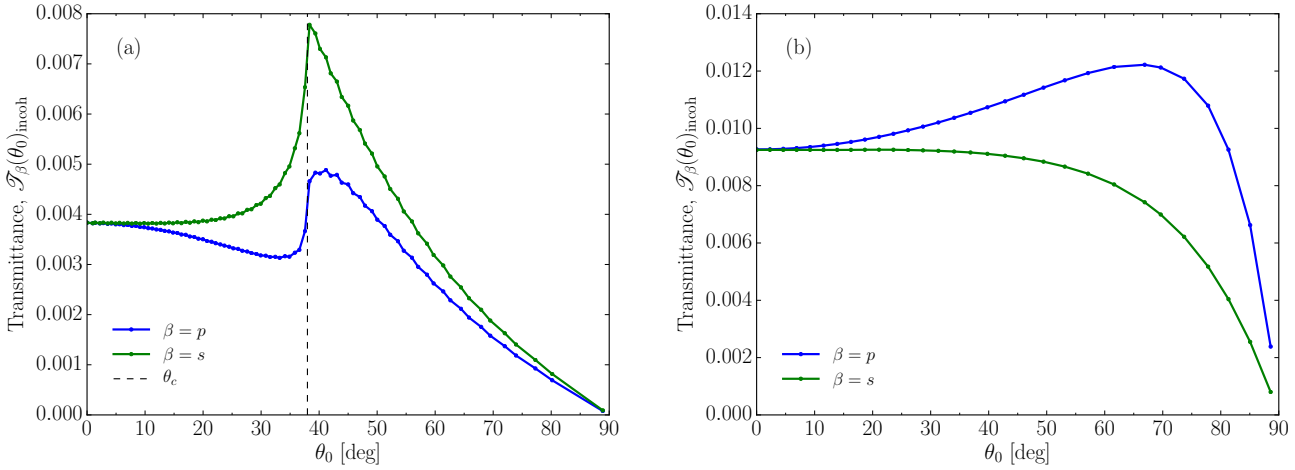

FIG. 12. The θ_0-dependence of the contribution to the transmittance from p- and s-polarized incident light that has been transmitted incoherently through a two-dimensional randomly rough surface. This quantity is for β-polarized incident light defined by the last term of Eq. (51), *i.e.* $\mathscr{T}_\beta(\theta_0)_{\rm incoh} = \mathscr{T}_\beta(\theta_0) - \mathcal{T}_\beta(\theta_0)$. The scattering systems assumed in obtaining these results were; (a) dielectric-vacuum ($\varepsilon_1 = 2.6869$, $\varepsilon_2 = 1$); and (b) vacuum-dielectric ($\varepsilon_1 = 1$, $\varepsilon_2 = 2.6869$). The critical angle θ_c' for total internal reflection for the flat dielectric-vacuum system is indicated by the vertical dashed line. The roughness parameters assumed were the same as in Fig. 2. Several simulations were run with small perturbations in the surface length L in order to obtain transmittance data with higher angular resolution (indicated by the solid dots).

$\mathscr{T}_\beta(\theta_0)_{\rm incoh}$ ($\beta = p, s$) are hence slowly varying functions of the angles of incidence consistent with what is observed in Fig. 12(b).

D. Accuracy of the simulations

Investigating the energy conservation of our simulation results can be a useful test of their accuracy. In combining simulation results from the current work with corresponding results obtained for the mean differential reflection coefficient $\langle \partial R_{\alpha\beta}/\partial \Omega_s \rangle$ through the use of the computationally similar methods from [2], we may add the total reflected and transmitted power for any lossless system. When the reflectance is added to the transmittance for any of the systems investigated in the current work, it is found that the results of these calculations satisfy unitarity with an error smaller than 10^{-4}. This testifies to the accuracy of the approach used, and it is also a good indicator for satisfactory discretization. It should be noted, however, that unitarity is a necessary, but not sufficient, condition for the correctness of the presented results. Through a preliminary investigation, unitarity seemed to be satisfied to a satisfactory degree for surfaces with a root mean square roughness up to about four times larger than the roughness used in obtaining the results presented in this paper.

VII. CONCLUSIONS

Needs to be polished We have presented a derivation of the reduced Rayleigh equations for the transmission amplitudes of light scattered from a two-dimensional, randomly rough, surface. These equations represent a non-perturbative, purely numerical solution of the scattering problem based on the Rayleigh hypothesis. As an example of their implementation in software, the full angular distribution for both co- and cross-polarized incoherent components of the mean differential transmission coefficients (MDTC) were reported, for configurations of vacuum and an absorptionless dielectric with a Gaussian surface power spectrum. It was shown that a configuration of transmission into a denser medium leads to Yoneda peaks: a peak in the incoherent MDTC at the critical angle for total internal reflection in the denser medium. Small amplitude perturbation theory, to lowest order in the surface profile function, was shown to reproduce our results qualitatively to a high degree of accuracy, both through analytical arguments and a numerical implementation of said theory. This lead us to believe that the features presented in the results are single-scattering effects.

As an investigation of the quality of the results, unitarity in energy conservation was found to be satisfied within 10^{-4} when the total scattered energy from both reflection and transmission was added together, for the roughness

parameters and configurations used in this paper.

Calculations of the transmission of light through two-dimensional randomly rough surfaces are challenging, and hence such they are still often carried out by means of perturbative and approximate methods. Our approach, through the reduced Rayleigh equations, represents a step towards more accurate but still computationally viable solutions of the problem.

VIII. TODO

- Comment on similarities and differences with our discussion vs the one by Kawanishi.
- We use two different θ_c even if they have the same value; should we define θ_c and θ_c' instead in order to not make any confusion (or maybe $\theta_t^\star$ and $\theta_0^\star$ showing that it is in different media)?
- Give more of the pert. theory expressions. Should these maybe go into the theory section? Check references to equation B2 and similar.
- Define $d_\alpha(k_\parallel)$ in terms of the polar angle on incidence and base the discussion partly on this.
- Question: Should we use Yoneda peaks in the title?
- Read the manuscript carefully with the intention of spotting duplication of statements and missing information.
- Update the conclusions and abstract.

Appendix A: Evaluation of $\mathbf{V}(\gamma|\mathbf{Q}_\parallel)$

In this appendix we outline the calculation of the vector $\mathbf{V}(\gamma|\mathbf{Q}_\parallel)$ defined by Eq. (16a). From Eqs. (16a) and (17) it follows immediately that

$$V_3(\gamma|\mathbf{Q}_\parallel) = I(\gamma|\mathbf{Q}_\parallel). \tag{A1}$$

The remaining two components of $\mathbf{V}(\gamma|\mathbf{Q}_\parallel)$ can be obtained by expanding $\exp\left(-\mathrm{i}\gamma\zeta(\mathbf{x}_\parallel)\right)$ in powers of the surface profile function and integrating the resulting series term-by-term ($\alpha = 1, 2$)

$$\begin{aligned}
V_\alpha(\gamma|\mathbf{Q}_\parallel) &= -\int \mathrm{d}^2x_\parallel\ \exp\left(-\mathrm{i}\mathbf{Q}_\parallel\cdot\mathbf{x}_\parallel\right)\exp\left[-\mathrm{i}\gamma\zeta(\mathbf{x}_\parallel)\right]\zeta_\alpha(\mathbf{x}_\parallel)\\
&= -\int \mathrm{d}^2x_\parallel\ \exp\left(-\mathrm{i}\mathbf{Q}_\parallel\cdot\mathbf{x}_\parallel\right)\zeta_\alpha(\mathbf{x}_\parallel)\sum_{n=0}^{\infty}\frac{(-\mathrm{i}\gamma)^n}{n!}\zeta^n(\mathbf{x}_\parallel)\\
&= -\sum_{n=0}^{\infty}\frac{(-\mathrm{i}\gamma)^n}{(n+1)!}\int \mathrm{d}^2x_\parallel\ \exp\left(-\mathrm{i}\mathbf{Q}_\parallel\cdot\mathbf{x}_\parallel\right)\frac{\partial\zeta^{n+1}(\mathbf{x}_\parallel)}{\partial x_\alpha}\\
&= -\frac{\mathrm{i}}{\gamma}\sum_{m=1}^{\infty}\frac{(-\mathrm{i}\gamma)^m}{m!}\int \mathrm{d}^2x_\parallel\ \exp\left(-\mathrm{i}\mathbf{Q}_\parallel\cdot\mathbf{x}_\parallel\right)\frac{\partial\zeta^m(\mathbf{x}_\parallel)}{\partial x_\alpha}.
\end{aligned} \tag{A2}$$

Introducing the Fourier representation of the mth power of the surface profile function,

$$\zeta^m(\mathbf{x}_\parallel) = \int\frac{\mathrm{d}^2P_\parallel}{(2\pi)^2}\,\hat\zeta^{(m)}(\mathbf{P}_\parallel)\exp\left(\mathrm{i}\mathbf{P}_\parallel\cdot\mathbf{x}_\parallel\right), \qquad m\geq 1, \tag{A3}$$

into Eq. (A2), and evaluating the two integrals after changing their order, results in

$$\begin{aligned}
V_\alpha(\gamma|\mathbf{Q}_\parallel) &= \frac{Q_\alpha}{\gamma}\sum_{m=1}^{\infty}\frac{(-\mathrm{i}\gamma)^m}{m!}\hat\zeta^{(m)}(\mathbf{Q}_\parallel)\\
&= \frac{Q_\alpha}{\gamma}\left[\sum_{m=0}^{\infty}\frac{(-\mathrm{i}\gamma)^m}{m!}\hat\zeta^{(m)}(\mathbf{Q}_\parallel) - (2\pi)^2\delta(\mathbf{Q}_\parallel)\right]\\
&= \frac{I(\gamma|\mathbf{Q}_\parallel)}{\gamma}Q_\alpha - (2\pi)^2\,\delta\left(\mathbf{Q}_\parallel\right)\frac{Q_\alpha}{\gamma}.
\end{aligned} \tag{A4}$$

In the last step we have used the result that

$$I(\gamma|\mathbf{Q}_\parallel) = \sum_{n=0}^{\infty} \frac{(-\mathrm{i}\gamma)^n}{n!} \hat{\zeta}^{(n)}(\mathbf{Q}_\parallel) \tag{A5}$$

and $\hat{\zeta}^{(0)}(\mathbf{Q}_\parallel) = (2\pi)^2 \delta\left(\mathbf{Q}_\parallel\right)$. Equation (A5) follows readily from Eq. (17) by expanding the latter in powers of the surface profile function and integrating the resulting series term-by-term.

By combining Eqs. (A1) and (A4) we arrive at the final result

$$\mathbf{V}(\gamma|\mathbf{Q}_\parallel) = \frac{I(\gamma|\mathbf{Q}_\parallel)}{\gamma} \left(\mathbf{Q}_\parallel + \gamma \hat{\mathbf{x}}_3\right) - (2\pi)^2 \, \delta\left(\mathbf{Q}_\parallel\right) \frac{\mathbf{Q}_\parallel}{\gamma}. \tag{A6}$$

We note that the last term of Eq. (A6), due to the presence of the factor $\delta\left(\mathbf{Q}_\parallel\right) \mathbf{Q}_\parallel$, will contribute only if $\mathbf{Q}_\parallel = \mathbf{0}$ implies that also γ must be zero; in all other cases this term will vanish. For this reason, we will refer to the second term of Eq. (A6) as the singular contribution to $\mathbf{V}(\gamma|\mathbf{Q}_\parallel)$.

Technically, $\mathbf{V}(\gamma|\mathbf{Q}_\parallel)$ is a distribution [20]; for instance, for the special case $\zeta(\mathbf{x}_\parallel) = 0$ it follows from Eq. (16) that $\mathbf{V}(\gamma|\mathbf{Q}_\parallel) = (2\pi)^2 \delta\left(\mathbf{Q}_\parallel\right) \hat{\mathbf{x}}_3$ (which is independent of γ). As is true for any distribution, it cannot appear alone in a mathematical expression and should therefore not be evaluated for a single argument as if it were an ordinary function; instead a distribution can only be evaluated after being multiplied by some (test) function. This has the consequence that the singular term of $\mathbf{V}(\gamma|\mathbf{Q}_\parallel)$ may not necessarily lead to a "real" singularity when evaluating the distribution. We will indeed see that this is what happens in our case.

Appendix B: Expansion of $T(\mathbf{q}_\parallel|\mathbf{k}_\parallel)$ in powers of the surface profile function

In this Appendix we outline the derivation of Eq. (52). We begin with the expansions

$$I(\gamma|\mathbf{Q}_\parallel) = \sum_{n=0}^{\infty} \frac{(-\mathrm{i}\gamma)^n}{n!} \hat{\zeta}^{(n)}(\mathbf{Q}_\parallel), \tag{B1}$$

where

$$\hat{\zeta}^{(n)}(\mathbf{Q}_\parallel) = \int \mathrm{d}^2 x_\parallel \, \mathrm{e}^{-\mathrm{i}\mathbf{Q}_\parallel \cdot \mathbf{x}_\parallel} \zeta^n(\mathbf{x}_\parallel) \tag{B2a}$$

$$\hat{\zeta}^{(0)}(\mathbf{Q}_\parallel) = (2\pi)^2 \, \delta\left(\mathbf{Q}_\parallel\right), \tag{B2b}$$

and

$$\mathbf{T}(\mathbf{q}_\parallel|\mathbf{k}_\parallel) = 2\alpha_1(k_\parallel) \sum_{n=0}^{\infty} \frac{(-\mathrm{i})^n}{n!} \mathbf{t}^{(n)}(\mathbf{q}_\parallel|\mathbf{k}_\parallel). \tag{B3}$$

In this latter equation the superscript n denotes the order of the corresponding term in powers of $\zeta(\mathbf{x}_\parallel)$. When Eqs. (B1) and (B3) are substituted into Eq. (26), the latter becomes

$$\begin{aligned} \sum_{m=0}^{\infty} \sum_{n=0}^{m} \frac{(-\mathrm{i})^m}{m!} \binom{m}{n} \int \frac{\mathrm{d}^2 q_\parallel}{(2\pi)^2} \left[-\alpha_1(p_\parallel) + \alpha_2(q_\parallel)\right]^{n-1} \hat{\zeta}^{(n)}(\mathbf{p}_\parallel - \mathbf{q}_\parallel) \mathbf{M}(\mathbf{p}_\parallel|\mathbf{q}_\parallel) \, \mathbf{t}^{(m-n)}(\mathbf{q}_\parallel|\mathbf{k}_\parallel) \\ = (2\pi)^2 \delta\left(\mathbf{p}_\parallel - \mathbf{k}_\parallel\right) \frac{1}{\varepsilon_2 - \varepsilon_1} \mathbf{I}_2. \end{aligned} \tag{B4}$$

When we equate terms of zero order in $\zeta(\mathbf{x}_\parallel)$ on both sides of this equation we obtain

$$\frac{1}{-\alpha_1(p_\parallel) + \alpha_2(p_\parallel)} \mathbf{M}(\mathbf{p}_\parallel|\mathbf{p}_\parallel) \, \mathbf{t}^{(0)}(\mathbf{p}_\parallel|\mathbf{k}_\parallel) = (2\pi)^2 \delta\left(\mathbf{p}_\parallel - \mathbf{k}_\parallel\right) \frac{1}{\varepsilon_2 - \varepsilon_1} \mathbf{I}_2. \tag{B5}$$

With the aid of the relation

$$\frac{1}{-\alpha_1(p_\parallel) + \alpha_2(p_\parallel)} = \frac{\alpha_1(p_\parallel) + \alpha_2(p_\parallel)}{(\omega/c)^2 \left(\varepsilon_2 - \varepsilon_1\right)}, \tag{B6}$$

Eq. (B5) can be rewritten in the from

$$\begin{pmatrix} \frac{1}{\sqrt{\varepsilon_1\varepsilon_2}}\left[\varepsilon_2\alpha_1(\mathbf{p}_\parallel)+\varepsilon_1\alpha_2(\mathbf{p}_\parallel)\right] & 0 \\ 0 & \alpha_1(\mathbf{p}_\parallel)+\alpha_2(\mathbf{p}_\parallel) \end{pmatrix} \begin{pmatrix} t_{pp}^{(0)}(\mathbf{p}_\parallel|\mathbf{k}_\parallel) & t_{ps}^{(0)}(\mathbf{p}_\parallel|\mathbf{k}_\parallel) \\ t_{sp}^{(0)}(\mathbf{p}_\parallel|\mathbf{k}_\parallel) & t_{ss}^{(0)}(\mathbf{p}_\parallel|\mathbf{k}_\parallel) \end{pmatrix} = (2\pi)^2\delta\left(\mathbf{p}_\parallel-\mathbf{k}_\parallel\right)\mathbf{I}_2, \tag{B7}$$

from which we obtain

$$\begin{pmatrix} t_{pp}^{(0)}(\mathbf{q}_\parallel|\mathbf{k}_\parallel) & t_{ps}^{(0)}(\mathbf{q}_\parallel|\mathbf{k}_\parallel) \\ t_{sp}^{(0)}(\mathbf{q}_\parallel|\mathbf{k}_\parallel) & t_{ss}^{(0)}(\mathbf{q}_\parallel|\mathbf{k}_\parallel) \end{pmatrix} = (2\pi)^2\delta\left(\mathbf{q}_\parallel-\mathbf{k}_\parallel\right) \begin{pmatrix} \frac{\sqrt{\varepsilon_1\varepsilon_2}}{\varepsilon_2\alpha_1(\mathbf{k}_\parallel)+\varepsilon_1\alpha_2(\mathbf{k}_\parallel)} & 0 \\ 0 & \frac{1}{\alpha_1(\mathbf{k}_\parallel)+\alpha_2(\mathbf{k}_\parallel)} \end{pmatrix}. \tag{B8}$$

For $m \geq 1$, Eq. (B4) can be written as

$$\begin{aligned} &\frac{1}{-\alpha_1(p_\parallel)+\alpha_2(p_\parallel)}\mathbf{M}(\mathbf{p}_\parallel|\mathbf{p}_\parallel)\mathbf{t}^{(m)}(\mathbf{p}_\parallel|\mathbf{k}_\parallel) + \int\frac{\mathrm{d}^2q_\parallel}{(2\pi)^2}\left[-\alpha_1(p_\parallel)+\alpha_2(q_\parallel)\right]^{m-1}\hat{\zeta}^{(m)}(\mathbf{p}_\parallel-\mathbf{q}_\parallel)\mathbf{M}(\mathbf{p}_\parallel|\mathbf{q}_\parallel)\,\mathbf{t}^{(0)}(\mathbf{q}_\parallel|\mathbf{k}_\parallel) \\ &\qquad + \sum_{n=1}^{m-1}\binom{m}{n}\int\frac{\mathrm{d}^2q_\parallel}{(2\pi)^2}\left[-\alpha_1(p_\parallel)+\alpha_2(q_\parallel)\right]^{n-1}\hat{\zeta}^{(n)}(\mathbf{p}_\parallel-\mathbf{q}_\parallel)\mathbf{M}(\mathbf{p}_\parallel|\mathbf{q}_\parallel)\,\mathbf{t}^{(m-n)}(\mathbf{q}_\parallel|\mathbf{k}_\parallel) = \mathbf{0}. \end{aligned} \tag{B9}$$

If we use the result that the matrix $\mathbf{M}(\mathbf{p}_\parallel|\mathbf{p}_\parallel)$ is diagonal and hence easily inverted, and that the matrix $\mathbf{t}^{(0)}(\mathbf{q}_\parallel|\mathbf{k}_\parallel)$ is given by Eq. (B8), we can simplify Eq. (B9) into

$$\begin{aligned} \mathbf{t}^{(m)}(\mathbf{p}_\parallel|\mathbf{k}_\parallel) =& -\left(\varepsilon_2-\varepsilon_1\right)\left[-\alpha_1(p_\parallel)+\alpha_2(k_\parallel)\right]^{m-1}\hat{\zeta}^{(m)}(\mathbf{p}_\parallel-\mathbf{k}_\parallel) \begin{pmatrix} \frac{\sqrt{\varepsilon_1\varepsilon_2}}{d_p(p_\parallel)} & 0 \\ 0 & \frac{1}{d_s(p_\parallel)} \end{pmatrix} \begin{pmatrix} \frac{\sqrt{\varepsilon_1\varepsilon_2}M_{pp}(\mathbf{p}_\parallel|\mathbf{k}_\parallel)}{d_p(k_\parallel)} & \frac{M_{ps}(\mathbf{p}_\parallel|\mathbf{k}_\parallel)}{d_s(k_\parallel)} \\ \frac{\sqrt{\varepsilon_1\varepsilon_2}M_{sp}(\mathbf{p}_\parallel|\mathbf{k}_\parallel)}{d_p(k_\parallel)} & \frac{M_{ss}(\mathbf{p}_\parallel|\mathbf{k}_\parallel)}{d_s(k_\parallel)} \end{pmatrix} \\ &-\left(\varepsilon_2-\varepsilon_1\right)\sum_{n=1}^{m-1}\binom{m}{n}\int\frac{\mathrm{d}^2q_\parallel}{(2\pi)^2}\left[-\alpha_1(p_\parallel)+\alpha_2(q_\parallel)\right]^{n-1}\hat{\zeta}^{(n)}(\mathbf{p}_\parallel-\mathbf{q}_\parallel) \\ &\qquad\times \begin{pmatrix} \frac{\sqrt{\varepsilon_1\varepsilon_2}M_{pp}(\mathbf{p}_\parallel|\mathbf{q}_\parallel)}{d_p(p_\parallel)} & \frac{\sqrt{\varepsilon_1\varepsilon_2}M_{ps}(\mathbf{p}_\parallel|\mathbf{q}_\parallel)}{d_p(p_\parallel)} \\ \frac{M_{sp}(\mathbf{p}_\parallel|\mathbf{q}_\parallel)}{d_s(p_\parallel)} & \frac{M_{ss}(\mathbf{p}_\parallel|\mathbf{q}_\parallel)}{d_s(p_\parallel)} \end{pmatrix} \mathbf{t}^{(m-n)}(\mathbf{q}_\parallel|\mathbf{k}_\parallel), \end{aligned} \tag{B10}$$

where

$$d_p(p_\parallel) = \varepsilon_2\alpha_1(p_\parallel)+\varepsilon_1\alpha_2(p_\parallel) \tag{B11a}$$

$$d_s(p_\parallel) = \alpha_1(p_\parallel)+\alpha_2(p_\parallel). \tag{B11b}$$

Equation (B10) allows $\mathbf{t}^{(m)}(\mathbf{p}_\parallel|\mathbf{k}_\parallel)$ to be obtained recursively in terms of $\mathbf{t}^{(m-1)}(\mathbf{p}_\parallel|\mathbf{k}_\parallel)$, …, $\mathbf{t}^{(1)}(\mathbf{p}_\parallel|\mathbf{k}_\parallel)$.

When $m = 1$, we obtain from Eq. (B10) the result

$$\mathbf{t}^{(1)}(\mathbf{q}_\parallel|\mathbf{k}_\parallel) = -\left(\varepsilon_2-\varepsilon_1\right)\hat{\zeta}^{(1)}(\mathbf{q}_\parallel-\mathbf{k}_\parallel) \begin{pmatrix} \frac{\varepsilon_1\varepsilon_2 M_{pp}(\mathbf{q}_\parallel|\mathbf{k}_\parallel)}{d_p(q_\parallel)d_p(k_\parallel)} & \frac{\sqrt{\varepsilon_1\varepsilon_2}M_{ps}(\mathbf{q}_\parallel|\mathbf{k}_\parallel)}{d_p(q_\parallel)d_s(k_\parallel)} \\ \frac{\sqrt{\varepsilon_1\varepsilon_2}M_{sp}(\mathbf{q}_\parallel|\mathbf{k}_\parallel)}{d_s(q_\parallel)d_p(k_\parallel)} & \frac{M_{ss}(\mathbf{q}_\parallel|\mathbf{k}_\parallel)}{d_s(q_\parallel)d_s(k_\parallel)} \end{pmatrix}. \tag{B12}$$

The matrix elements $\left\{M_{\alpha\beta}(\mathbf{q}_\parallel|\mathbf{k}_\parallel)\right\}$ are given by Eq. (27a).

In view of Eq. (B3) we find that through terms linear in the surface profile function

$$\begin{aligned} \mathbf{T}(\mathbf{q}_\parallel|\mathbf{k}_\parallel) =& (2\pi)^2\delta\left(\mathbf{q}_\parallel-\mathbf{k}_\parallel\right) \begin{pmatrix} \frac{\sqrt{\varepsilon_1\varepsilon_2}}{d_p(k_\parallel)} & 0 \\ 0 & \frac{1}{d_s(k_\parallel)} \end{pmatrix} 2\alpha_1(k_\parallel) \\ &+ \mathrm{i}(\varepsilon_2-\varepsilon_1)\hat{\zeta}^{(1)}(\mathbf{q}_\parallel-\mathbf{k}_\parallel) \begin{pmatrix} \frac{\varepsilon_1\varepsilon_2 M_{pp}(\mathbf{q}_\parallel|\mathbf{k}_\parallel)}{d_p(q_\parallel)\,d_p(k_\parallel)} & \frac{\sqrt{\varepsilon_1\varepsilon_2}M_{ps}(\mathbf{q}_\parallel|\mathbf{k}_\parallel)}{d_p(q_\parallel)\,d_s(k_\parallel)} \\ \frac{\sqrt{\varepsilon_1\varepsilon_2}M_{sp}(\mathbf{q}_\parallel|\mathbf{k}_\parallel)}{d_s(q_\parallel)\,d_p(k_\parallel)} & \frac{M_{ss}(\mathbf{q}_\parallel|\mathbf{k}_\parallel)}{d_s(q_\parallel)\,d_s(k_\parallel)} \end{pmatrix} 2\alpha_1(k_\parallel) + \mathcal{O}\left(\zeta^2\right). \end{aligned} \tag{B13}$$

The substitution of these results into Eq. (41) and using $\langle\hat{\zeta}(\mathbf{Q}_\parallel)\hat{\zeta}(\mathbf{Q}_\parallel)^*\rangle = S\delta^2 g(|\mathbf{Q}_\parallel|)$ yields Eq. (52).

ACKNOWLEDGMENTS

The research of Ø.S.H. and I.S. was supported in part by The Research Council of Norway Contract No. 216699. This research was supported in part by NTNU and the Norwegian metacenter for High Performance Computing (NOTUR) by the allocation of computer time.

---

[1] I. Simonsen, J. B. Kryvi, A. A. Maradudin, and T. A. Leskova, Comput. Phys. Commun. **182**, 1904 (2011).
[2] T. Nordam, P. A. Letnes, and I. Simonsen, Frontiers in Physics **1**, 1 (2013).
[3] T. A. Leskova, P. A. Letnes, A. A. Maradudin, T. Nordam, and I. Simonsen, **8172**, 817209 (2011).
[4] J.-J. Greffet, Phys. Rev. B **37**, 6436 (1988).
[5] T. Kawanishi, H. Ogura, and Z. L. Wang, Waves in Random Media **7**, 351 (1997).
[6] Y. Yoneda, Physical review **131** (1963).
[7] G. Renaud, R. Lazzari, and F. Leroy, Surf. Sci. Rep. **64**, 255 (2009).
[8] A. Soubret, G. Berginc, and C. Bourrely, Physical Review B **63**, 245411 (2001).
[9] C. Yeh, Phys. Rev. E **48**, 1426 (1993).
[10] W. Press, S. Teukolsky, W. Vetterling, and B. Flannery, *Numerical Recipes: The Art of Scientific Computing*, 3rd ed. (Cambridge University Press, 2007).
[11] A. A. Maradudin, T. Michel, A. R. McGurn, and E. R. Mendez, Ann. Phys. **203**, 255 (1990).
[12] I. Simonsen, J. B. Kryvi, A. A. Maradudin, and T. A. Leskova, Comp. Phys. Commun. **182**, 1904 (2011).
[13] Make a comment about what $\hat{\mathbf{k}}_{\parallel}$ is when $\mathbf{k}_{\parallel} = 0$.
[14] T. Nordam, P. A. Letnes, I. Simonsen, and A. A. Maradudin, Journal of the Optical Society of America A **31**, 1126 (2014).
[15] I. Simonsen, A. A. Maradudin, and T. A. Leskova, Phys. Rev. A **81**, 013806 (2010).
[16] T. A. Leskova, P. A. Letnes, A. A. Maradudin, T. Nordam, and I. Simonsen, Proc. Int. Soc. Opt. Eng. **8172**, 817209 (2011).
[17] I. Simonsen, A. A. Maradudin, and T. Leskova, Phys. Rev. Lett. **104**, 223904 (2010).
[18] P. A. Letnes, A. A. Maradudin, T. Nordam, and I. Simonsen, Phys. Rev. A **86**, 031803 (2012).
[19] T. Nordam, P. A. Letnes, I. Simonsen, and A. A. Maradudin, Opt. Express **20**, 11336 (2012).
[20] I. M. Gelfand and G. E. Shilov, *Generalized Functions, Volume I: Properties and Operations* (Academic Press, New York, 1964).